heritage

MDPI

Article

How Could Increasing Temperature Scenarios Alter the Risk of Terrorist Acts in Different Historical Squares? A Simulation-Based Approach in Typological Italian Squares

Enrico Quagliarini, Gabriele Bernardini * and Marco D'Orazio

DICEA, Università Politecnica delle Marche, Via Brecce Bianche 12, 60131 Ancona, Italy; e.quagliarini@staff.univpm.it (E.Q.); m.dorazio@staff.univpm.it (M.D.)
* Correspondence: g.bernardini@univpm.it; Tel.: +39-0712204246

Abstract: Squares in the urban historical built environment are public open spaces prone to the risk of terrorist acts, essentially because they are ideal soft targets and attract significant user densities. Risk assessment methods should consider how users behave in them, both before and during an accident (i.e., the evacuation process). In addition to squares' morphology and layout, and considering that urban areas are more and more prone to the effects of increasing temperatures, outdoor climate conditions can alter the initial scenario. In fact, such conditions can lead users to gather in specific outdoor areas, where they can look for shadows and shelter. This work hence proposes a simulation-based approach to assess how differences in users' behaviours in response to increasing temperatures and squares' morphology can alter the risk of terrorist acts in an emergency evacuation. An agent-based model is developed to simulate the interactions between users, hazards and the historical built environment. The work considers four typological squares prone to terrorist acts since they host a special building attracting users in front of it. These squares are derived from the analysis of Italian historical contexts within the BE S^{2}ECURe project. Users are generated in the public open space (thus, before the terrorist act) depending on the intended uses of the square and on the outdoor temperature, which is affected by the square's morphology. Three different users' behaviours are modelled to consider (or not) the effects of the outdoor temperature on users' thermal acceptability levels in an increasing temperature situation. Then, two evacuation scenarios are simulated: (a) a general evacuation process, without attackers, as the baseline for the risk assessment; and (b) an armed assault with cold weapons, to define one of the most probable attack situations in open spaces. Evacuation performance indicators are developed to assess users' risk. Preliminary verifications demonstrate the capabilities of the approach. The results show that higher differences in evacuation indicators are noticed in large and asymmetric squares, since their conditions highly affect the variability of users' behaviours in response to increasing temperatures. At the same time, stronger safety behaviours in response to increasing temperatures could reduce emergency issues because they allow users to be more dispersed and initially placed farther from the attack area. Decision-makers could take advantage of the proposed approach and simulation tool, moving towards an effectiveness analysis of solutions to increase the thermal comfort of users in respect of the risk levels during an evacuation. Finally, applications to real-world scenarios are thus encouraged to compare such idealized results with effective conditions.

Keywords: historical built environment; squares; built environment typologies; evacuation simulation; terrorist acts; increasing temperatures; public open spaces

Citation: Quagliarini, E.; Bernardini, G.; D'Orazio, M. How Could Increasing Temperature Scenarios Alter the Risk of Terrorist Acts in Different Historical Squares? A Simulation-Based Approach in Typological Italian Squares. *Heritage* **2023**, *6*, 5151–5186. https://doi.org/10.3390/heritage6070274

Academic Editors: Humberto Varum, Vasilis Sarhosis and Fernanda Prestileo

Received: 30 May 2023
Revised: 26 June 2023
Accepted: 3 July 2023
Published: 6 July 2023

1. Introduction

Historical squares are public open spaces in the urban built environment and fundamental parts of the urban tangible cultural heritage [1,2]. They are significant attractors of users to our historical cities, given their social and cultural functions [3–5], thus being

affected by high potential risk levels in case of an emergency [6–9] due to a natural or anthropogenic disaster [10].

In fact, squares can collect a high number of users, including visitors to building heritage, monuments, urban sights and pedestrian areas, thus increasing the exposure [11] with respect to the surrounding urban fabric [9]. Such users have different features (e.g., age, gender, motion abilities), attend to several tasks in the built environment, and have different behaviours, habits and levels of familiarity with the built environment [3,12–14], thus also influencing individual vulnerability [11]. Furthermore, squares can be affected by high physical vulnerability in view of the characteristics of the building heritage, urban infrastructure, outdoor layout and interaction with the urban form, since they are parts of the historical city as a whole [10,15]. Finally, the attraction of users can increase the probability that an emergency related to an anthropogenic disaster could occur [8,16,17].

In particular, squares can be identified as potential "soft targets" prone to terrorist acts [7,16–19]. They can be classified as public open spaces with "low or no security against violent attacks and attraction for the attacker" due to the aforementioned high exposure [16]. Data from the Global Terrorism Database (https://www.start.umd.edu/gtd/, accessed on 18 April 2023) relating to the years from 2000 to 2020 outline that about 12% of attacks have been carried out in public squares and plazas, being comparable to attacks in "hard targets" such as military barracks and similar facilities. The maximization of the impacts that can be achieved by a terrorist act in a square is influenced by the possibility of "inflicting fear to the population and attaining media coverage" [18]. Furthermore, additional (over)crowd accidents could appear due to crowd gathering and dynamics [8], thus increasing the risks for the users also in emergency and evacuation conditions.

A terrorist act in a public open space such as a historical square could imply that users have to evacuate the space where they are initially placed, especially if no protection-in-place measures could be performed [19–22]. In this case, users placed outdoors should leave the square and move towards the linked streets [23–25].

The risk for the square's users hence depends on both the direct effects of the attack on people and the evacuation process, thus highlighting the importance of assessing the interactions between the users, the built environment and the hazard conditions from a behavioural standpoint, as is typical for other kinds of sudden-onset emergencies (e.g., fires) [26,27]. The analysis of terrorist act-related emergencies should hence consider the combination of the following:

- The morphological features and construction technologies of the built environment elements composing and delimiting the square, also in correlation with the urban fabric, to effectively identify factors concerning the physical vulnerability. The morphology and the layout of a square are constant elements to be considered regardless of the attack type because they affect the distribution of the users and their movement in the evacuation process [19,22]. Construction technologies and specific building components implemented in the square layout could be relevant in the case of specific attack types [17,19,22,28]. For instance, permanent barriers can be useful against vehicle attacks, and the adopted construction technologies are important to evaluate blast vulnerability and related effects in terms of damages, although their impact is negligible in case of attacks with cold weapons.
- The possible use over space and time due to the hosted functions, and the related users' behaviours, to take into account the background scenario, that is, before the terrorist act, and the users' exposure and vulnerability. It depends on the boundary conditions concerning the intended uses of the areas [3,9], but also on the microclimate-related factors [14,29]. In particular, historical urban built environments are more and more prone to increasing temperature phenomena, leading to the possibility of critical outdoor conditions and thermal stress for users [15,30]. Users can then adapt their behaviours and distribution in public open spaces depending on individual outdoor thermal acceptability, open space landscapes and the presence of other mitigative elements such as shaded areas, canopies, and so on [29,31,32].

- The hazards that can strike the built environment and the needs and behaviours of users and stakeholders during an emergency. Considering terrorist acts, the related issues should be based on the possible types of attacks that can occur in a given scenario and on the emergency scenario in terms of the behaviours adopted by the attackers and the users [23,33–38]. As a consequence, it allows the inclusion of response issues and moving towards the analysis of coping capacity, resistance and resilience.

Emergency evacuation simulation models could be used to support this process [39], since they can reproduce the complexities of the interactions among these elements. A similar approach to risk assessment is widely supported in the case of other kinds of disasters, such as earthquakes, fires and floods, at both the single-building and urban scales, and it is also applied to historical built environment contexts [10,40–43]. Previous approaches to terrorist act evacuation simulators have been developed in recent years and could be used to support risk assessment and evaluate how specific scenarios could impact the users' risk [44–47]. Nevertheless, their current limitations relate to the fact that they are mainly oriented to buildings rather than to public open spaces. Thus, to the best of the authors' knowledge, the combined influence of the morphological features, the use of the open spaces depending on the boundary conditions, including the ones relating to microclimate-related features, and the typology of the attack have been not properly investigated.

1.1. Work Aims, Research Questions and Contribution Outlines

In view of the above, the general work aims of this contribution are aimed at investigating how users' behaviours in response to outdoor (increasing) temperatures can alter the risks due to terrorist act evacuation for the users of public historical squares.

In detail, four typological squares prone to terrorist acts are considered to derive different relevant morphological conditions. These typologies have been previously derived from the analysis of real-world Italian historical urban public squares within the BE S^2ECURe project [48], and they have already been used to investigate increasing temperature conditions [30]. As for previous applications of simulation models [42,43,48–54], the typological (and thus "idealized") open spaces investigated in this work represent archetypes of real-world squares and, in such a way, can provide quick and general insights at a broader perspective in respect to specific case studies.

Users' behaviours towards climate-related scenarios, as expressed in terms of outdoor temperatures (i.e., UTCI), are simulated in respect of experimental-based criteria in relation to thermal acceptability outdoors [29]. In this sense, they can change the distribution of users outdoors, which is mainly due to the hosted functions of the public square [9]. Three thermal acceptability levels are modelled. The first considers that users are placed in a sort of "no increasing temperature" scenario and they are always placed outdoors in comfort conditions, thus assuming that the local temperature does not alter the users' distribution. The second and third scenarios are influenced by the outdoor temperature according to an increasing temperature situation, depending on two thermal (i.e., transient and 1 h) acceptability ranges.

Considering the different "modus operandi" and attack typologies of terrorists [19], attacks with cold weapons, such as swords or knives, or, in a more general way, sharp objects seem to be one of the more probable scenarios in countries where hot weapons are generally strictly forbidden [44]. Research also pointed out an increase in the use of such weapons in recent years [55]. Thus, this kind of attack is considered in the current work, although scenarios studying the evacuation process without the attackers are also performed to have a comparison baseline of the phenomena [47].

On such bases, a simulation model relying on agent-based modelling and cellular automata [38,39,44,56] is developed and then applied to combinations of the aforementioned input factors. The users' initial distribution depends on the square's morphology and the outdoor users' thermal behaviours. Then, the simulation of the emergency evacuation in

case of a terrorist act is offered according to previous quick but reliable approaches and experimental-based data [23,36–38,57,58].

Considering the general work aims and the selected variables, the following specific research questions have been addressed:

1. "Do the climate-related effects on users alter the risk, considering the same morphology and attack scenario?"
2. "Do the climate-related effects and morphology alter the risk under the same attack scenario?"
3. "Does the attack scenario with cold weapons increase users' risks with respect to the conditions without the attackers?"

In this context, the work is associated with the general workflow of the project titled BE S^2ECURe ("Built Environment Safer in Slow and Emergency Conditions through behavioUral assessed/designed Resilient solutions", funded by the Italian Ministry of Education, University, and Research). The BE S^2ECURe project aims at developing methods for risk assessment and mitigation in crowded open spaces, focusing on historical squares, and evaluating the combined impact of built environment features, other boundary conditions related to climate change and anthropogenic hazards (i.e., increasing temperatures and pollution), emergency conditions implying evacuation (i.e., terrorist acts and earthquakes) and users' behaviours. Previous works were devoted to (a) the identification of typological scenarios of risk-prone built environments based on the analysis of real-world squares [48], (b) the simulation-based analysis of their outdoor conditions in the case of increasing temperatures [30,59], and (c) the identification of the main terrorist risk factors in squares [7,19]. This contribution moves towards the next required step concerning the analysis of the joint effects of these elements on the users' risk during the evacuation process and hence traces the methodological bases for specific case study applications.

The remainder of this paper is structured as follows. Related works are provided in Section 2. The description of the assessed scenarios and of the simulation model is resumed in Section 3. The simulation results are offered in Section 4, while Section 5 outlines the main work contributions and limitations.

2. Related Works

According to the general outlines in Section 1 and the work aims, the main related works concern typologies of squares prone to terrorist acts in the reference context of this work, that is, Italy (Section 2.1); users' behaviours in response to outdoor temperatures affecting their distribution in the public squares because of individual thermal acceptability (Section 2.2); and terrorist act behaviours and evacuation simulation (Section 2.3).

2.1. Typologies of Squares Prone to Terrorist Acts in the Italian Context

Previous works pointed out how the analysis of the risk conditions of public open spaces in the historical built environment, mainly squares, should be based on reliable scenario creation in terms of the physical features, hazards and users' exposure and social/individual vulnerability [48,60,61]. Some efforts in terms of simulation-based risk assessment in a specific public open space in the urban built environment have been carried out [60,62,63]. However, squares are limitedly investigated in this sense.

Performing an analysis on Built Environment Typologies (BETs), and thus on square archetypes, could speed up the process. For instance, considering other research contexts, research-defined inventories of buildings and urban mesh typologies for historical urban scenarios to support widespread conservation tasks [64], risk assessments and mitigations [50–54], or energy, air quality and comfort performances [59,65–67]. In this context, morphology and its classifications have been consolidated [48,68–71], e.g., according to a statistical or parametric description of the built environment features. The analysis of such typological, archetypical and, thus, "general" scenarios has significant informative outcomes, especially at the broadest scale. In fact, using specific case studies could reduce the efficiency and effectiveness of simulation-based approaches, since it needs time-consuming

modelling of the specific scenarios, and the results are quite hard to generalise also in view of the fact that historical urban contexts (such as open spaces and squares) were built organically over time. On the contrary, decision-makers, such as public local authorities, and their technicians should be supported by quick methodologies for risk assessment, such as those relying on typological scenarios [48]. Nevertheless, the use of typological scenarios can generate preliminary outcomes that could be then "tailored" to the specificities of each case study.

Recent activities in the BE S^2ECURe project were able to define BETs representing clusters of historical squares [48], as relevant public open spaces in historical city centres. Five BETs are derived from the analysis of a large database composed of more than 1000 real-world historical squares in Italy by also combining each of them with the related main risks to which they are prone. In particular, considering the risk of terrorist acts and, in particular, cold weapons attacks, as identified in Section 1.1, the main BET physical vulnerability parameters and risk-affecting parameters are essentially related to the following:

- The presence of a special building, that is, a building hosting a special function, thus including building heritage, i.e., places of worship, public buildings, educational buildings, and cultural and tourism attractions. In fact, these strategic and symbolic targets, characterized by significant crowding conditions in view of the hosted functions and sights, are ideal soft targets for terrorists [3,6,24].
- The morphology of the square and, mainly, its layout, dimensions and shape, as well as the features of its access streets. In fact, when an attack occurs in a square, users could leave it by moving towards the access streets and could be potentially exposed to behavioural interferences from crowding and attack risk conditions [19,46].

The historical square morphology also alters the outdoor built environment conditions modifying the local outdoor temperature and shaded areas, also in combination with the radiative features, due to the employed materials and the presence of greenery [15,32,72].

Moreover, the typological users' exposure and vulnerability were retrieved by adopting the same experimental-based approach to a sample of historical squares in the same Italian context [9]. Statistical data on the functions hosted in the square (open spaces and buildings), on user densities, and on users' typologies (e.g., depending on age and gender) have been retrieved to describe the recurrent conditions of such historical squares.

Previous works investigated the outdoor temperature profiles in the BETs to provide a simulation-based assessment of the heat stress due to increasing temperatures [30], demonstrating the capabilities of the typological approach in deriving general criticalities. Nevertheless, efforts to assess the risk of terrorist acts and the evacuation process in the BETs contexts are still needed. It is worth noticing that, although the retrieved BETs and typological data are developed starting from the analysis of squares in Italian historical cities, the method used for the definition of the BETs can be applied to other national/international contexts. Furthermore, the approach has been applied to the clustering of squares into BETs, although it could be applied to any other public open space in historical scenarios.

Simulation-based approaches have been applied to assess the impact of the built environment morphology using typological configurations for different emergency and evacuation scenarios, mainly by focusing on single buildings (i.e., to test the impacts of typological layouts and dimension variations on fire safety and to provide preliminary validation of models) [42,49] or even urban open spaces [52–54]. Conversely, squares have not been investigated.

2.2. Users' Thermal Acceptability in Open Spaces

Users' behaviours in public open spaces are highly affected by the environmental stressors characterizing the microclimatic conditions [14,31,62,72]. Increasing temperatures can lead to critical conditions in the microclimate, and they are mainly relevant in urban built environments, including squares and, more in general, all the historical public open spaces, because they are essentially influenced by [14,15,32,48,73]: (a) the building construc-

tion materials; (b) the morphological and geometric features of open spaces, including the height of the facing buildings; and (c) the general poor implementation of green areas and blue infrastructures and shadings in open spaces.

Previous works underlined that users can reduce their attendance of open spaces in critical conditions, such as those of increasing temperatures or poor air quality [14,74]. Nevertheless, leisure and social activities can still encourage permanence in the outdoors (especially in specific conditions, such as during holidays, mass gatherings, and for physical activities [14,75,76]), and specific dynamics of users' distribution in the outdoors are then activated. Although some outdoor attractive areas in the outdoors can still exist, users can adapt their position by looking for areas with lower temperatures, minimizing the outdoor permanence time, and moving towards shaded areas. Such behaviours depend on thermal comfort issues, which affect the individual acceptable temperature range [32]. Previous works defined experimental criteria for users' permanence in outdoor areas according to the Universal Thermal Climate Index (UTCI) and to their permeance time in open spaces [29]. This work identified two thermal acceptability behaviours and defined experimental-based correlations between the UTCI and users' thermal acceptability probability (*PA*) [%]. The transient one relates to short-time permanence in the outdoor spaces (e.g., for passersby) and implies higher *PA* values than the ones of the 1 hour behaviour, which relates to higher permanence time (e.g., for users performing social and leisure times outdoors). Then, the 1 hour behaviour implies that pedestrians become more sensible to the UTCI while selecting their position in the open space and, majorly, to increasing temperatures. Nevertheless, cultural effects and individual features, as well as the geographical context, impact the users' behaviour and the acceptability range, making the users' response more significant, especially in open spaces where temperature variations are consistently distributed and in the hot seasons [14,32]. In this sense, Mediterranean areas as well as temperate and warm climates are relevant examples, such as those considered in this work [30,31,71].

Although studies on thermal stress in historical open spaces have been performed, including squares as relevant scenarios [15,30,32,59,77], the impacts of these conditions on users' distribution in the public open space is not yet analysed in correlation with possible evacuation scenarios, such as those due to terrorist acts.

2.3. Evacuation Behaviours and Simulation Models in the Terrorist Act Context

Human behaviours during terrorist acts have been defined to be implemented in emergency simulators [33,34]. The main approaches used to derive behavioural tasks concern interviews with survivors of real-world attacks [78,79], empirical studies on real-world events [23,35] and, more recently, virtual reality-based studies [80]. In detail, recent efforts were aimed at assessing the most probable behaviours according to the analysis of real-world events by aggregating all the collected data and dividing them by specific contexts, i.e., in terms of the type of attack and built environment in which the event occurred (indoor versus outdoor) [23]. Such work also provided a specialization of the fundamental diagram of pedestrian dynamics for evacuations following terrorist acts, thus overcoming the limits of other approaches that adopt general diagrams in simulations.

Different simulation models have been derived, mainly by pursuing a microscopic approach to represent the interactions between the specific elements and users in the scenario [81]. These models are generally based on cellular automata [38,44], which divides the scenario into cells, and the social force model [36,47,82,83], which is essentially connected to a continuous representation of the environment. Moreover, agent-based modelling has been implemented to provide different types of users and related specific actions to be performed [36,37,82–85]. In addition to the simulation of the attackers' and evacuees' behaviours, some works provided the possibility to represent trained evacuation leaders as specific agents in the simulation [36,85], as well as to include counterforce measures by police [81].

In general terms, these models provide different patterns of the attackers' movements in respect of the evacuees, mainly pointing out the prey (the evacuees)–predator (the

attackers) model and shortest distance strategy [47,57,83]. In particular, for the shorter distance strategy, the prey are the nearest pedestrians to the attacker. Considering that each weapon used by the terrorists has an attack range [36–38], they can become a casualty in case they are placed at a distance shorter than the attack weapon. Furthermore, models also included the probability of being found or suffering from the attack [57]. This shortest distance-based strategy can maximize the casualty rate. Thus, the higher the number of attackers, the higher the efficacy of the attack. According to such an approach, users try to move farther from the areas where the attackers are present and, thus, towards the safe areas (in a square, the linked streets) [57]. Perceived risk fields have been provided to this end by considering the highest values where the attackers are placed [37,38,47]. Such behaviour seems to be based on a simple but reliable approach, which is consistent with real-world noticed conditions in which people run far from the attack area [23] as well as with "run and hide" recommendations by law enforcement agencies [36].

Additional behavioural issues, such as "panic" effects, have been considered [44], although they are poorly related to the experimental-based data. Similarly, only a limited number of works performed validation activities using real-world contexts [46], essentially because of the difficulties of extracting data for the scenario creation in a reliable manner. Nevertheless, the adoption of consolidated standards on typological conditions (such as those of the IMO guidance) [42,86] could be exploited to encourage preliminary verifications.

From an implementation perspective, the cellular automata are well established and used, since they use 2D cells and grids to represent the built environment layout in a quick but reliable manner and hence consider good balancing with the execution timing. In this sense, they are also useful to perform massive evacuation simulations [40,87]. Many models were based on the use of NetLogo-based solutions [40,82,83], which easily combine agent-based modelling and cellular automata principles in simulations [56].

Most of these applications are oriented to buildings; however, in view of the above, applications to public open spaces are urgently needed to investigate the combined effects of morphological and climate-related factors, and they can take advantage of such a combined simulation approach.

3. Phases and Methods

This work is organized according to three phases, as traced in the general workflow shown in Figure 1. The first phase (Section 3.1) relates to the definition of the BET-based scenarios for the simulations [9,30,48]. Variations in the morphological and climate-related parameters of these ideal squares are represented with respect to a possible attack using cold weapons and a baseline scenario without attackers. This first phase also involves the definition of users' exposure and vulnerability, and it contributes to the creation of 24 input scenarios for the simulations. Then, the second phase (Section 3.2) concerns the development of a simulation model according to the agent-based and cellular automata approaches to represent the users' behaviours before and during a terrorist act with respect to the built environment and its morphology, the climate-related factors to consider comfort and increasing temperature scenarios, and the attack. The third phase (Section 3.3) finally involves running the simulations and their comparisons thanks to key performance indicators oriented to users' behaviours during an evacuation. Specific statistical tests are also performed to evaluate the differences between the scenarios (Section 3.4).

The notations used in the sections are also listed and described in Appendix A, Table A1.

3.1. BET-Based Scenarios for Simulations: Selection of Combination of Morphology, Climate-Related Scenario, Terrorist Act and Users' Exposure and Vulnerability

Four BETs are selected in this work as archetypes of Italian historical squares. As remarked in Section 2.1, their features are based on the statistical analysis of a large sample of real-world squares in the Italian context according to previous works by the research

group [48]. In the same work, these squares were also associated with their probable hazard conditions. They were also used by previous research within the BE S^2ECURe project concerning the analysis of microclimatic scenarios in case of increasing temperatures [30,59]. The same context of Italian historical squares has been also used to support the definitions of the typologies in terms of users' exposure and vulnerability [9]. Table 1 presents a list of the configurations for each of these assumed factors, while the specific conditions are illustrated in the following subsections. Their combinations allow the creation of 24 input scenarios for the simulations performed using the model described in Section 3.2 and the analysis criteria shown in Section 3.3. It is worth underlining that no mitigation solutions are considered in the simulated scenarios, as pointed out in Table 1.

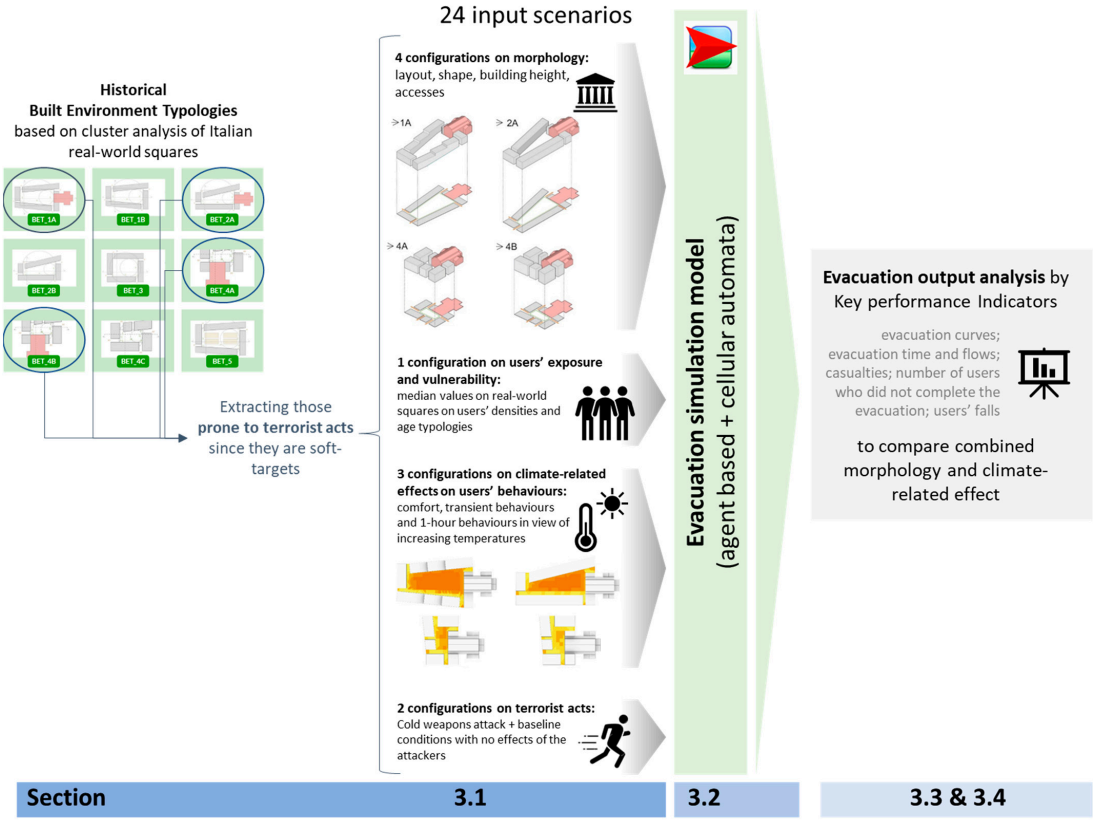

Figure 1. General research workflow and correlation with the following methodological sections for each of the work phases (authors' elaboration of the BET views and heatmaps from [30,48]).

Table 1. List of the configurations for each of the assumed factors: morphology, users' exposure and vulnerability, climate-related scenario and terrorist act. Codes are used in Section 3 in the interest of brevity.

Morphology	Users' Exposure and Vulnerability	Climate-Related Scenario [Code]	Terrorist Act [Code]
BET1A BET2A BET4A BET4B	Overall number of exposed users = 625 pp; users waiting outdoors to enter the special buildings = 480 pp; age percentage = 4% toddlers, 9% parent-assisted child, 6% young adults, 64% adults, 18% elderly	No effects of UTCI, as in users' thermal comfort [E] Moderate UTCI effects on users' distribution outdoors before the evacuation, related to the Milan climate (daytime from 11:00 till 16:00 in summer day) [M] Significant UTCI effects on users' distribution outdoors before the evacuation, related to the Milan climate (daytime from 11:00 till 16:00 in summer day) [S]	No attackers [A] Cold weapon attack; attackers placed in the area where users are waiting to enter the special building [W]

3.1.1. BET Morphology

Four morphological configurations have been investigated in this work, one for each BET. Figure 2 shows the plans, sections and axonometric views of the investigated BETs and thus outlines the recurrent conditions of the plan dimensions, ground elevation, built front height, number of access streets, and presence of at least a special building that can be the main soft target within the square. Considering the overall Italian historical squares database used to derive these BETs [48], the considered BETs represent the archetypes of more than 60% of the whole investigated sample.

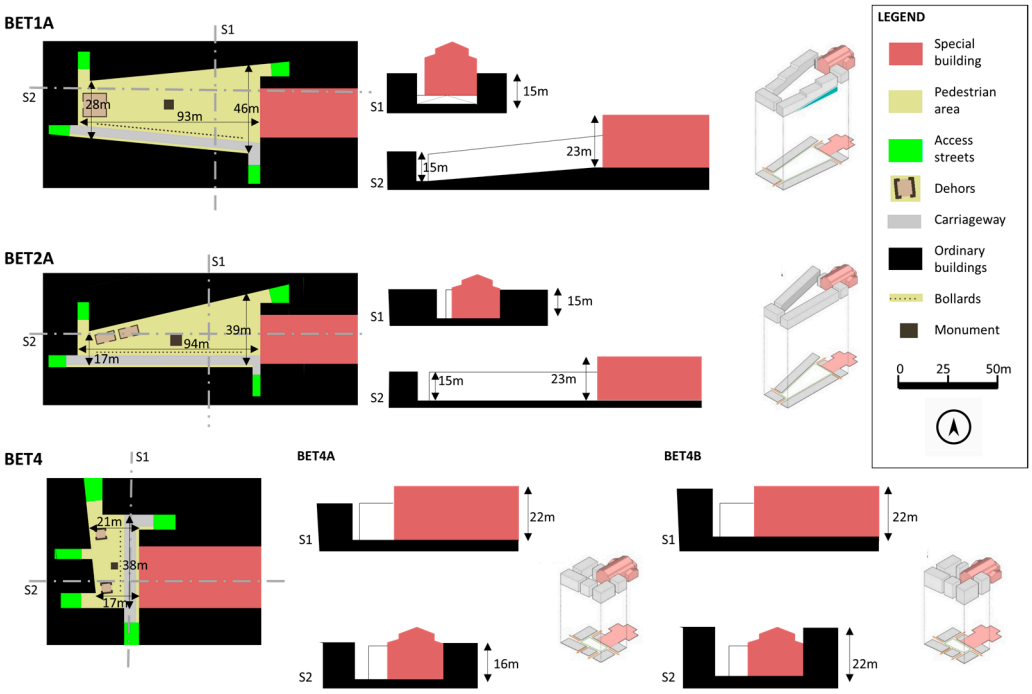

Figure 2. Plans, sections and axonometric views of the BETs considered in this work, as derived by [48]. Legend, metric scale and north direction as shown in the top right corner. Access streets are 4 m to 6 m (i.e., for carriageways) wide.

All the BETs share some common features. They are characterized by the absence of shadings, canopies and green areas, thus indicating possible critical outdoor conditions in case of increasing temperatures [30]. Most of their outdoor area is represented by pedestrian areas (light yellow in Figure 2). Dehors, such as the outdoor areas of a bar or a restaurant (light brown area in Figure 2), are placed in this public open space, and they are considered as bordered by a fixed barrier, which always has an overall area of 100 m^2. A carriageway crosses the square, having a width of 4 m (light grey area in Figure 2). A monument (e.g., a statue or a fountain, 6 m × 6 m) is placed at the centre of the square, and poles are located along the carriageway, at a distance of about 7 m from the nearest built front, to delimit the main pedestrian area (dark brown in Figure 2). These poles can represent punctual elements such as fixed bollards or light poles [22]. The monument and the poles are considered outdoor obstacles in the evacuation process, while no impact on the users' distribution at the simulation's start is considered in view of the no shading effects. The access streets are considered evacuation targets in case of evacuation due to terrorist acts (green area in Figure 2). The median surface of the special buildings is equal to 1200 m^2 in each BET, and a religious intended use could be reasonably assumed for it (i.e., a church) [9].

In detail, BET2A (pedestrian and dehors area of about 2400 m^2) has the lowest level of compactness and regularity among the considered BETs (ratio between the minimum width and length of about 0.18), while BET4A and BET4B (pedestrian and dehors area of about 700 m^2) have the highest levels in this sense (ratio between the minimum width and length of about 0.44). BET1A (pedestrian and dehors area of about 3000 m^2) is mainly

characterized by a symmetry axis and a funnel shape, associated with a ground slope of about 8%. BET4B has the highest ratio between the built front height and the minimum square width (about 1.30), while all the other BETs are described by a value of this ratio < 1. In this sense, BET4B is characterized by the widest shaded areas, thus slightly limiting the outdoor temperature thanks to its morphology with respect to the other BETs [30].

3.1.2. Users' Exposure and Vulnerability

Typological conditions concerning users' exposure and vulnerability in the square are derived from previous works [9]. The adopted configuration refers to recurring holiday conditions from 11:00 to 16:00, which can imply the opening of the special buildings (i.e., a church, according to Section 3.1.1) and are consistent with the climate scenario described in Section 3.1.3. According to the work aims, the terrorist act affects public open spaces, and thus users placed indoors do not participate in the evacuation process nor are they affected by emergency effects [20]. This assumption is consistent with a cold weapon attack [19,44].

To make the scenarios comparable in terms of the involved users, the same number of users has been considered for all the BETs. In particular, 625 persons are considered as initially placed outdoors according to experimental-based median values of the user density [9]. In addition to passersby (generated in pedestrian areas) and dehors users (generated in dehors areas), users of the special building in the BET, which is assumed as a church, are generated in front of it to consider that they are involved in leisure or social tasks, waiting to enter and visit the special building, or waiting for the religious functions [9,14]. This choice relies on a conservative approach to terrorist act analysis since it maximises the number of exposed users who can be directly affected by the attack while being placed outdoors. Details of the user number calculation are reported in Appendix B. Concerning the users' vulnerability, five classes have been modelled to consider the typologies of users by age, as this individual feature influences the users' motion speed and abilities [9,88]. These classes have been associated with the percentages of users according to statistics about historical squares in Italy [9] as follows:

- Toddlers (0 to 4 years) directly depend on their parents to move: 4%.
- Parent-assisted children (5 to 14 years) can autonomously move but they are generally strictly influenced by their parents: 9%.
- Young users (15 to 19 years) have the highest motion speeds according to age–speed correlations: 5%.
- Adults (20 to 69 years): 64%.
- Elderly (70+ years) are characterized by sensible possible reduced motion speed and abilities in respect of adults: 18%.

Although the elderly are contemplated in the assessed scenarios, we would like to point out that no specific adaptation or risk mitigation measures implemented depending on the users' age requirements are implemented in the BETs due to their general features as well as to the work aims [48].

3.1.3. Climate-Related Scenarios

Three climate-related scenarios are modelled for each BET to represent the effects on users' behaviours derived from the literature works [29,30,32] as follows:

1. No effects of the UTCI (code E in Table 1): All the users placed outdoors are considered in comfort conditions.
2. Moderate effects of the UTCI (code M in Table 1): Behaviours of passersby and users waiting to enter the special buildings are associated with transient thermal acceptability, while behaviours of dehors users are associated with 1 hour thermal acceptability since they are considered more sensitive to heat compared to the others.
3. Significant effects of the UTCI (code S in Table 1): Behaviours of passersby are associated with transient thermal acceptability, while behaviours of users of dehors and users waiting to enter the special buildings are associated with 1-h thermal acceptabil-

ity. In this case, users waiting to enter the special buildings are considered as sensitive to heat as all the other users who are placed outdoors for a longer time.

The first scenario hence refers to the baseline conditions, that is, no increasing temperature effects, while the second and third scenarios can represent the effects of increasing temperatures on the users' distribution [30]. Details of the equations for the user distribution generation according to acceptability probability for each behaviour are illustrated in Section 3.2. The second and third scenarios are derived using the outdoor UTCI values for each BET, which depend on the built environment radiative features and the climate context. To this end, the current work uses the methodology provided by previous research on typological risks in increasing temperature scenarios performed during the BE S^2ECURe project [30].

All the BET are characterized by radiative features (i.e., surface type, reflectance) derived according to previous classification works for Italian historical squares [48] and to the previous application of the BET to the increasing temperature risk assessment [30]. In particular, the reflectance values considered for the UTCI assessment in all the BETs are 0.7 for the rook, 0.5 for the façade, and 0.08 for asphalt surfaces.

The climate context of Milan (Italy) is selected for all the BETs according to previous work by the research group [30]. This climate is representative of many northern cities in Italy and Central Europe according to emergency events databases about extreme temperatures [89]. In statistical terms, more than 50% of the square samples investigated using the proposed typological approach to users' exposure and vulnerability [9] refer to northern cities in Italy. Furthermore, most of the historical city centres placed in this geographical area are also tourist destinations, and thus these squares can become ideal soft targets for terrorist acts [16,17] or even be affected by (over)crowd accidents [8] (e.g., as in the Piazza San Carlo accident in Turin in 2017).

Figure 3 overlaps the UTCI map to the plan of each of the assessed BET within the Milan climate context, considering daytime from 11:00 till 16:00 in the hottest week of the year, during summer. This choice implies obtaining the most critical conditions for the users placed outdoors.

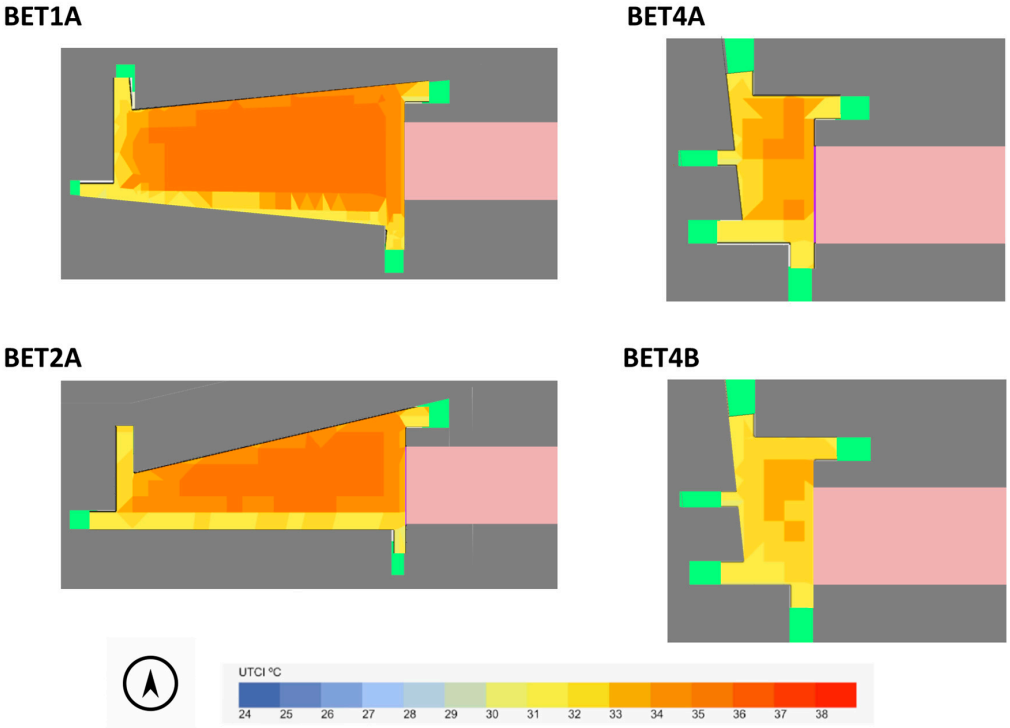

Figure 3. UTCI [°C] scheme (from 11:00 till 16:00) of the BETs (colour map on the bottom), as shown on the BET morphology and layout plan. Data are derived from [30].

These maps have been derived from previous work within the project [30] using ENVIMET simulations based on the climate scenarios, the radiative features and the morphology described above. In this reference work, the UTCI values have been calculated on a 5 m × 5 m grid representation of the BET, and standard ventilation conditions and other climate data concerning the Milan climate context have been used. A full discussion of the simulation approach is offered in [59]. Furthermore, in comparison with other reference climates in Italy (i.e., Rome, Aosta, Bolzano), the Milan climate is characterized by the worst effects in terms of the UTCI distributions [59]. Considering the BETs in Figure 3, for the Milan climate, BET4B refers to the lowest UTCI values in their distribution, ranging from about 30 to 33 °C. Indeed, BET1A is affected by the highest UTCI values (up to 36 °C), essentially because it is the widest one and has a low ratio between the built fronts height and square width. In view of the above, the UTCI values of each BET, as described in Figure 3, are uploaded into the simulator to generate the outdoor users' distribution before the evacuation for the scenarios involving moderate and significant UTCI effects on the users.

3.1.4. Terrorist Act

According to Section 2.1, the presence of a special building implies that the BET is prone to *terrorist acts* in view of its symbolic value and its potentially high number of hosted users [7,16,17]. According to the work aims, two kinds of evacuation scenarios are simulated in this work, and both of them imply the evacuation of the outdoor spaces of the square. Thus, users initially placed indoors do not need to participate in the evacuation process and can simply remain inside the buildings, where they are protected from the accident.

These two scenarios are as follows:

1. A scenario with "no attackers" (code A in Table 1) is first considered to replicate the baseline conditions in the square evacuation [47].
2. A scenario with the presence of attackers performing a terrorist act using cold weapons (code W in Table 1), according to the scheme in Figure 4. It is considered that the attack is performed where most of the users are gathering outdoors, thus in front of the church. In this scenario, a prey–predator attack approach is combined with the shortest distance strategy, and a casualty is provoked when the prey is inside the attack range of the predator [36,47,57,83]. To focus on users' safety assessment in the evacuation, and considering real-world users' responses and recommendations from law enforcement agencies [23,36], no fighting behaviours are considered in this work.

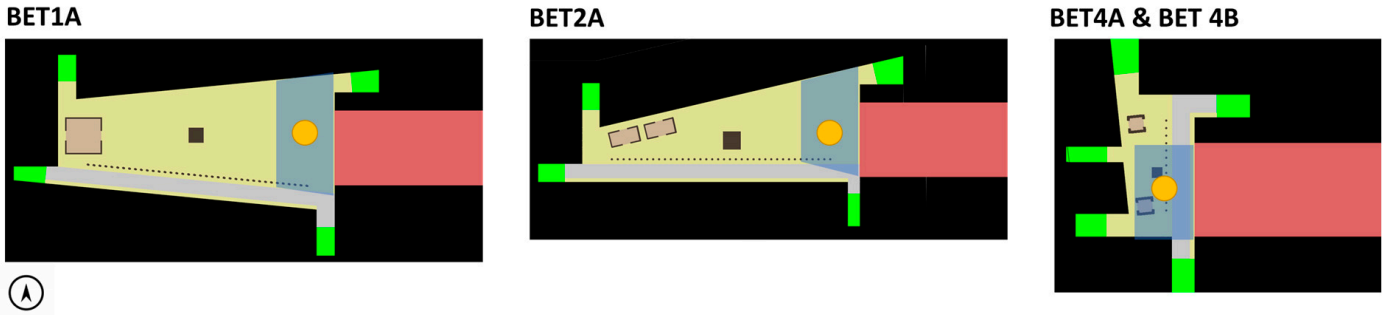

Figure 4. Scheme of the position of the attackers (yellow circle) and of the main areas where the users are waiting to enter the special building (transparent blue area) for each BET.

Figure 4 shows the scheme of the attackers' position (yellow circle) overlapped with the graphical representation of the BETs and with the position of the users waiting to enter the special building (transparent blue areas).

3.2. Evacuation Simulation Model: Definition and Implementation

According to previous approaches [40,43,56,82,83], the simulation model is developed according to agent-based modelling and cellular automata principles. The model is then implemented through the NetLogo platform [90] (version 6.2.0).

To translate the scenarios defined in Section 3.1, four main agents interacting in the simulation are defined: the *built environment*; the *users*, considered as evacuees; the *climate-related scenario*; and the *attackers*.

The built environment is described by its morphology according to the criteria expressed in Section 3.1.1. The *built environment*, where the *users* behave and move, is represented by squared cells (side: 50 cm), which are consistent with the user dimensions [43]. In this way, this approach ensures reduced calculation time with respect to continuous space representations, while it also guarantees a generally reliable prediction accuracy [38,40,44,56,87]. Each cell has specific features concerning the physical outdoor built environment: (a) an obstacle, a part of a building or a part of a special building, which cannot be occupied by the *users* and the *attackers* at the simulation start and while moving; and (b) a part of the outdoor area that is composed of pedestrian areas and dehors, where the *users* and the *attackers* are effectively generated at the simulation start and which can be used by them while moving and evacuating.

Furthermore, each cell has specific features with respect to the *climate-related scenario* in terms of the UTCI. These data are used to generate the *users'* distribution depending on the combination of the physical features of the outdoor built environment and the UTCI conditions, which are the considered drivers of the users' thermal acceptability, according to previous works [29,30]. In particular, users can be initially generated in cells that can be pedestrian areas or dehors (compare with Section 3.1.3). The probability of occupying a cell of the outdoor areas is expressed in terms of the thermal acceptability probability *PA* [%], which depends on the UTCI value of a given cell and is expressed according to Equation (1) [29]. In particular, Equation (1) shows the calculation of the transient probability *PAt* [%] and the 1 h probability *PAh* [%].

$$PA = \begin{cases} PAt = -0.086\ UTCI^2 + 4.019\ UTCI + 54.119 \\ PAh = -0.249\ UTCI^2 + 12.914\ UTCI - 85.681 \end{cases} \quad (1)$$

For each user, the *PA* is compared to a random number (uniform distribution of probability). In case the random value is lower than the *PA*, the user is generated in the current assessed cell according to the same probability. Otherwise, the user moves to another cell of the same type and the whole process is repeated.

After being generated in outdoor spaces, the terrorist act starts and the *users* try to evacuate the square by moving towards its access streets, which are the evacuation targets and far from the attackers, if present [36–38,47,57,83]. According to Section 3.1 and the work aims, the evacuation only involves the outdoor *users* because their positions can be directly affected by the accident [19,20,22]. The model is structured to include an individual premovement time (e.g., to consider their distance from the attack or possible delays in the terrorist act recognition) [23,58]. Nevertheless, in this work, this premovement time is set equal to 0 s to focus on the most critical movement conditions in the square due to the contemporary evacuation starting and since premovement time statistics for terrorist acts are not consolidated [23].

To simulate the *users'* movement, an affordance-based criteria approach [43] is adopted to create a dynamic floor field that can "describe the willingness to walk" of a user placed in a certain cell towards one of the evacuation targets [87]. At a given time t, each cell c has a given affordance $Aff_{c,t}$ [-], which essentially depends on the surrounding pedestrian density, the distance towards the evacuation target, the distance from the *attackers* (if present) and the distance from obstacles. The higher the $Aff_{c,t}$, the higher the probability that the *user* can select c. Meanwhile, the *attackers* try to move according to previous prey–predator logics (compare with Section 3.1.4) [47,57,83]. An attack range between the attacker and the evacuee [36–38] of a 1 m radius is assumed as the threshold for casualties. Nevertheless,

the proposed model also considers the probability that a user can be wounded [57], which is associated with the Terrorism Self-Aid Procedure (TSAP) probability threshold [%]. Users who are not wounded can evacuate, while the others are conservatively assumed as casualties. In this work, the TSAP is conservatively assumed equal to 50%.

The *users* are also classified into age typologies as described in Section 3.1.2. The impact of this classification essentially relates to the *users'* evacuation speed [58,88], which is calculated according to the adaptation of the fundamental diagram for pedestrian dynamics [91] based on experimental values concerning terrorist acts [23]. An individual random speed variation is also assigned [23,88]. The pedestrian density is also used to estimate the probability that physical contact among users can appear by implying users' falls and evacuation stops [58].

The simulation ends when the last alive *user* reaches an access street and exits from the square or when the maximum simulation time is reached. In this work, the maximum simulation time is equal to 150 s, which is about the maximum time needed to complete the evacuation of a user in minimum free-flow conditions (0.72 m/s [23]) along the longest path in the built environment due to $F_{d,c,t}$ (about 105 m, referring to BET1A).

A complete discussion of the evacuation simulation models is offered in Appendix C, while the preliminary verification tests of the model are reported in Appendix D.

3.3. Simulation Criteria and Key Performance Indicators for Risk Assessment

At least 10 simulations are performed for each scenario, verifying that the standard deviation of the evacuation time $\leq 5\%$, since this is selected as the main simulation goodness indicator [86]. In fact, the simulations are affected by stochastic effects related to the initial user distributions, speed calculation, cell selection and motion loops.

According to previous works' remarks [83], the statistical-based trends in the simulation outputs are hence calculated. First, the median evacuation curves, in terms of the number of users reaching an access street of the square over time, are assessed to depict the overall effects of the interactions between *users*, the *built environment* and the *attackers*. Median values are chosen since they are not easily affected by extreme data at each simulation step and because such output data can have a non-normal distribution [92].

Then, the key performance indicators are considered to assess the users' risk, taking advantage of suggestions from previous research on evacuation analyses for both terrorist acts and other kinds of emergencies affecting the built environment (e.g., general purposes, fires, earthquakes), including those related to typological applications [43,45,47,60,63,83,86,93]. The selected indicators range from 0 (safety) to 1 (risk), thus being expressed according to normalization rules and allowing comparison of the different input scenarios on the same scale of effects. As for the evacuation curves, the median values are calculated [92].

The normalized evacuation time *TN95* [-] is calculated as the ratio between the evacuation time of 95% of users who arrived at a safe area *T95* [s] and the maximum simulation time (in this work, 150 s, according to Section 3.2). The analysis of 95% of the users limits the impacts on the results due to "outliers" in reference to model uncertainties. The higher the *TN95*, the higher the risk, since *users* do not quickly abandon their initial hazardous position.

Starting from this value, the users' flow corresponding to the evacuation time of 95% of users who arrived at a safe area *F95* [pp/s] is compared to 1.5 pp/s/m as the maximum specific users' flow [91] to derive the normalized flows *FN95* [-] according to Equation (2). The higher the *FN95*, the lower the evacuation speediness, e.g., given the hosted *users'* number, thus the higher the risk.

$$FN95 = \max\left(0.1 - \frac{F95 \Big/ \sum \ access\ streets\ width}{1.5 pp/s/m}\right) \quad (2)$$

The normalized number of physical contacts among the users *PN* [-] is calculated in Equation (3) to compare the effective and maximum physical contacts over *T95*. The

normalization is performed on the 5% of users placed outdoors, since this is the reference probability threshold to stop the evacuation, as defined in Section 3.2 [58]. Dividing the number of events by *T95* ensures the comparison of different evacuation times and scenarios. The higher the *PN*, the stronger the effects of a dense crowd motion and obstacle interactions.

$$PN = \frac{\left(sum\ of\ physical\ contacts\ among\ users\ over\ T95 \Big/ T95 \right)}{5\%\ of\ exposed\ users} \quad (3)$$

The casualty ratio *CR* [-] is obtained as the ratio between the number of *user* casualties due to the attackers and the overall number of exposed *users*. The higher the *CR*, the higher the impact of the attackers. Thus, in the "no attackers" scenario, *CR* = 0. Furthermore, the percentage of users who did not complete the evacuation during the simulation time *NE* [-] is calculated with respect to the overall number of exposed *users*. The *NE* is affected by the built environment morphology and the attackers' strategy because it includes also the number of casualties, as discussed in detail in Section 3.2 and Appendix C.

The key performance indicators are traced for each scenario derived from the combination of configurations shown in Table 1, showing their distributions by using robust boxplot visualization [92]. Furthermore, the users' distribution at the start of the simulation because of the UTCI effects is also assessed in density terms for the significant BETs to better describe the related differences.

3.4. Statistical Tests

The following statistical tests on the key performance indicators are performed to solve the main research questions shown in Section 1.1 [92]:

1. To understand if "the climate-related effects on users alter the risk, considering the same morphology and attack scenario", such indicators have been aggregated by each BET and terrorist act scenario. Thus, for each BET morphology, the median percentage variations or each indicator are determined by separately comparing the results for the "moderate" and "significant effects of the UTCI" scenarios with those of the "no effects of the UTCI" scenarios. The significance of the test is evaluated by the Kruskal–Wallis test. This test is hence performed on 8 aggregate scenarios, considering independent groups within the same boundary conditions. The null hypothesis of the test is that, for each indicator, the sample data from the "no effect", "moderate" and "significant effects of the UTCI" scenarios come from the same distribution.
2. To understand if "the climate-related effects and morphology alter the risk under the same attack scenario", such indicators have been aggregated by the terrorist act scenario. Then, the Scheirer–Ray–Hare test is performed on 2 aggregate scenarios considering independent groups within the same attack conditions (i.e., no attackers, cold weapons). In this case, three groups of conditions for the BET morphology have been selected: (a) BET4A and BET 4B are merged since they have the same plan layout; (b) BET1A; and (c) BET2A. This non-parametric test is analogous of the parametric multi-factorial ANOVA. The null hypothesis is that there are no interactions between the factors. Then, Dunn's test is provided as a post-hoc test. The null hypothesis of this test is that no difference among the groups exists. In this case, no percentage variations in the median values have been introduced in view of the major differences among the BET morphology;
3. To understand if "the attack scenario with cold weapons increases users' risks with respect to the conditions without the attackers", the KPIs have been aggregated by each BET morphology and UTCT effects scenario. Then, the median percentage variations in each KPI are determined by comparing the results of the "cold weapon attack" scenario with respect to the ones of the "no attackers" scenarios. The significance of the test is evaluated again by the Kruskal–Wallis test. In this case, the null hypothesis

of the test is that, for each KPI, the sample data from the "cold weapon attack" and "no attackers" scenarios come from the same distribution.

For all the tests, *alpha* = 0.05 is selected. The tests have been carried out in MATLAB 2023a version (mathworks.com accessed on 25 June 2023), respectively using the kruskalwallis and SRH_test plus dunn functions (see, respectively, https://www.mathworks.com/matlabcentral/fileexchange/96399-non-parametric-alternative-of-2-way-anova-scheirerrayhare and https://github.com/dnafinder/dunn—MATLAB Central File Exchange, accessed on 15 May 2023). The selected non-parametric tests have been selected in view of the possible indicators of non-normality and heteroscedasticity, thus not supporting the use of ANOVA tests, including an n-ways ANOVA [92].

4. Results

This section first traces an overview of the key performance indicators to compare and contrast the general results according to the tested scenarios (Section 4.1). Then, the results of the statistical tests are used to solve the main research questions (Section 4.2).

4.1. Key Performance Indicators Overview

Figure 5 shows the comparisons of the evacuation curves considering the "no attackers" [A] and "cold weapon attack" [W] scenarios depending on the "no effects" [E], "moderate effects" [M] and "significant effects" [S] of the UTCI on the users' distribution and depending on the BET morphology, that is, BET1A (Figure 5A), BET2A (Figure 5B), BET4A (Figure 5C) and BET4B (Figure 5D).

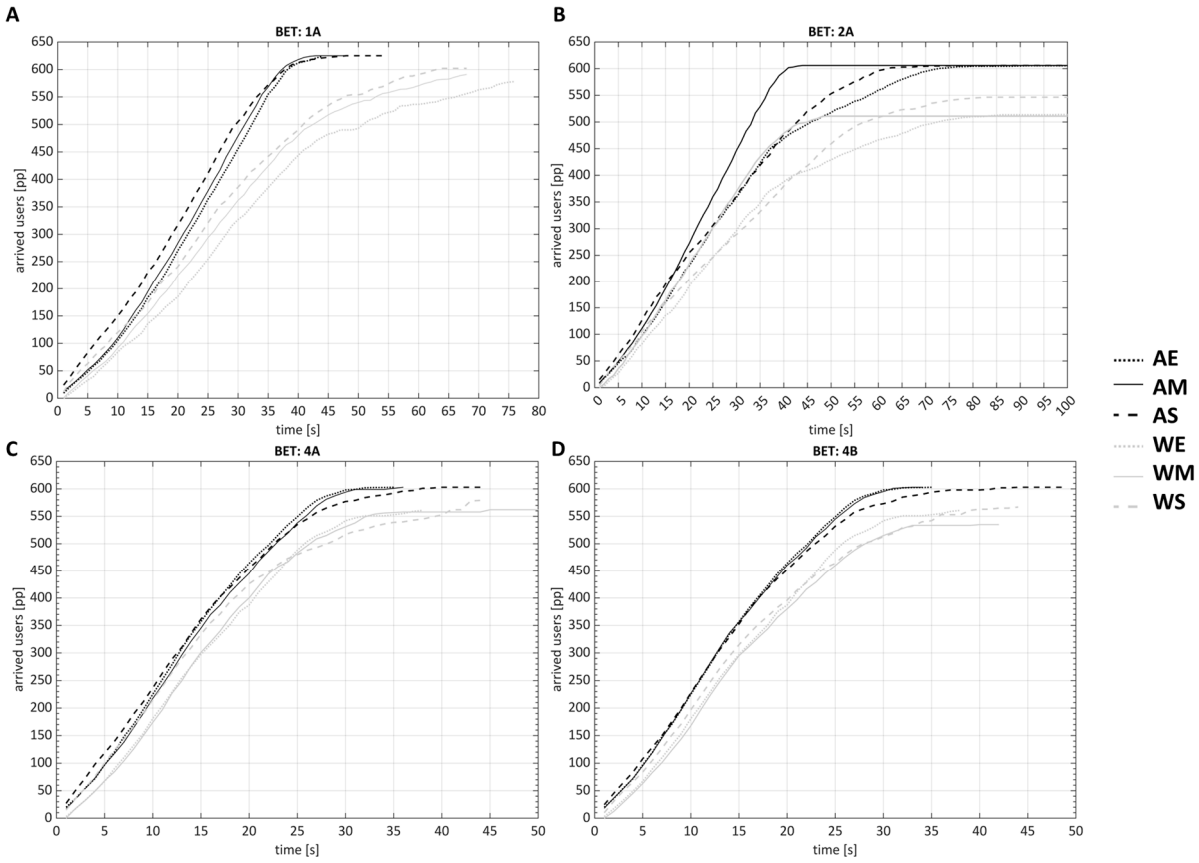

Figure 5. Evacuation curve comparisons considering the "no attackers" [A] and "cold weapon attack" [W] scenarios depending on the "no effects" [E], "moderate effects" [M] and "significant effects" [S] of the UTCI on the users' distribution and depending on the BET morphology: (**A**) BET1A, (**B**) BET2A, (**C**) BET4A and (**D**) BET4B. Codes refer to Table 1.

In all the BETs, these curves graphically highlight that the "cold weapon attack" scenarios are generally "slower" than the "no attackers" scenarios, which is as expected, since users should modify their evacuation process because of the interaction with the attackers according to the prey–predator adopted approach (Sections 3.1.4 and 3.2). Furthermore, the main difference between these two attack conditions refers to the number of evacuees who could complete the evacuation. This result is shown by the maximum y-axis value, which represents the number of arrived users [pp]. Thus, the BET morphology, as expected, does not alter this general trend, while it affects the graphical differences in the curves when considering the specific effects of the UTCI on the users' initial distribution (according to the roles reported in Sections 3.1.3 and 3.2). Nevertheless, in the most compact and regular BETs (i.e., BET4A and BET4B), such UTCI-related effects seem to graphically be slighter than in the wider and less regular BETs. Finally, the curves also point out that the "no effects of the UTCI" scenarios do not directly imply a graphical increase in the speediness of the evacuation process (i.e., referring to the slopes of the curves). At the same time, the speediness differences are less evident in the first part of the evacuation process (up to about 20 s), which is quite similar in all the scenarios. In fact, in this first part of the process, the users who arrived at the evacuation targets are those placed closest to them, and thus they also limitedly interact with the possible source of the attack. In this sense, this element essentially limits the impact of the combined scenario conditions.

Figures 6 and 7 trace the boxplot representations of the key performance indicators, that is, respectively, the *TN95*, *FN95*, *PN* and *CR* for Figure 6 and the NE for Figure 7. These boxplots are based on the simulation results aggregated by the considered scenarios due to the configuration combinations in Table 1.

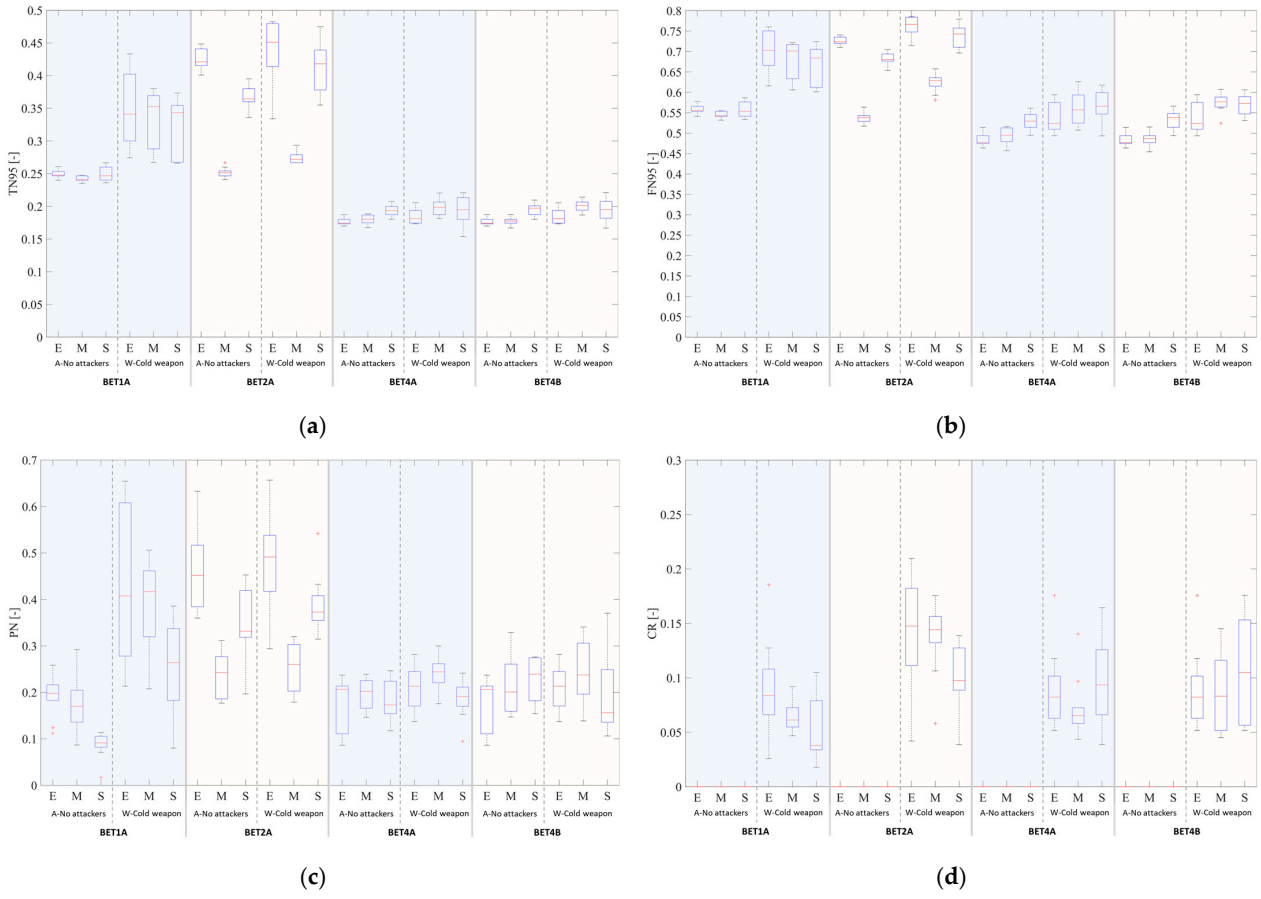

Figure 6. Boxplots of the key performance indicators by scenario combination in terms of the BET morphology (x-axis labels, last text row, in terms of BET), attack conditions (x-axis labels, central text row) and effects of the UTCI (x-axis labels, upper text row): (**a**) *TN95* [-]; (**b**) *FN95*; (**c**) *PN*; (**d**) *CR*. Codes refer to Table 1.

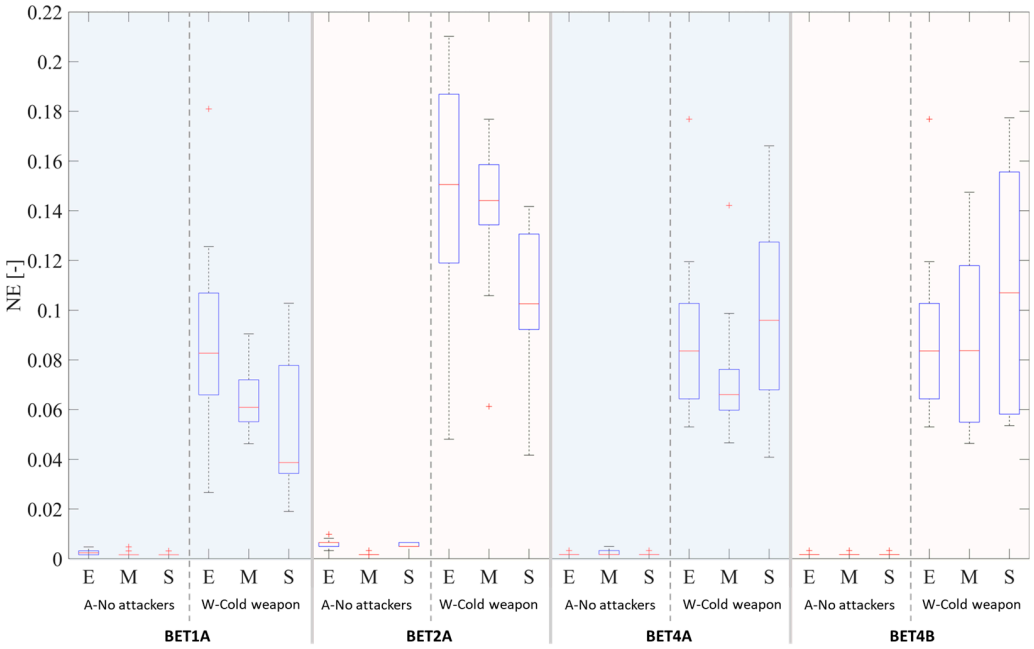

Figure 7. Boxplot of the *NE*[-] by scenario combination in terms of the BET morphology (x-axis labels, last text row, in terms of BET), attack conditions (x-axis labels, central text row) and effects of the UTCI (x-axis labels, upper text row). Codes refer to Table 1.

In detail, Figure 6a summarizes the boxplot visualization of the *TN95* for the simulation scenarios. Considering the vertical extension of the boxplots, it is possible to observe that a compact and regular BET morphology generally corresponds to smaller ranges of the boxplots, such as, mainly, for BET4A and BET4B, regardless of the attack and UTCI-effects scenarios. This phenomenon is essentially due to the lower spatial extension and complexity of these BETs, and it is matched with the considerations performed for Figure 5C,D. On the contrary, the presence of attackers in the "cold weapon attack" scenario can imply less convergent boxplots, such as in the case of BET1A and BET2B. This issue is generally due to the users' interactions with the attackers.

Figure 6b shows the *FN95* boxplots, thus relating to the users' flows and mediating the number of arrived users by T95. In general terms, this graph mainly points out that the *FN95* increases in the "cold weapon attack" conditions for all the BET morphology and the UTCI-effects scenarios because of the increase in the *TN95* and in the reduced number of arrived users provoked by casualties (compare with Figure 6d). Similarly, less convergent *FN95* boxplots are noticed for the "cold weapon attack" scenarios, thus remarking on the comments for Figure 6a. Nevertheless, the "no attackers" and "cold weapon attack" scenarios share the same general trends in the *FN95* boxplots for the three UTCI-effects conditions, especially in the scenarios with the most complex (i.e., BET2A) and most compact (i.e., BET4A) morphology.

Figure 6c traces the impacts of the physical contact probability over the considered scenarios by tracing the *PN* boxplots. In general terms, the median *PN* values are higher in the "cold weapon attack" conditions. Such a result suggests that users should adapt their movement against the prey–predator rules and that physical contacts and fall probabilities hence increase. As a consequence, this risk indicator increases too. Furthermore, the width of the boxplots is different considering the morphology and UTCI-effects scenarios. Considering the dispersion of the boxplots as a sort of output uncertainty, the less critical scenarios are those referring to BET4A and BET4B for the "cold weapon attack". This result could be affected by the regular and compact morphology of the square. Figure 8 integrates the analysis of the *PN* by showing the main areas where physical contacts among users can occur. As expected, most physical contacts occur at the entrance areas of the access streets and close to the corners where users' flow should move towards a confined space. In the

wider layout of BET1A and BET2B, such areas are more concentrated in those areas that are placed closer to the front of the special building, where most of the users are concentrated (compare also with Figure 9). In BET4A and BET4B, the most compact morphology also points out that additional points of contact appear near the dehors due to the overlapping effects of the movement of dehors users and the other pedestrians. The points shown in Figure 8 are representative of all the simulated configuration combinations in Table 1, while differences mainly exist in terms of the final *PN* outcomes, as shown by Figure 6c.

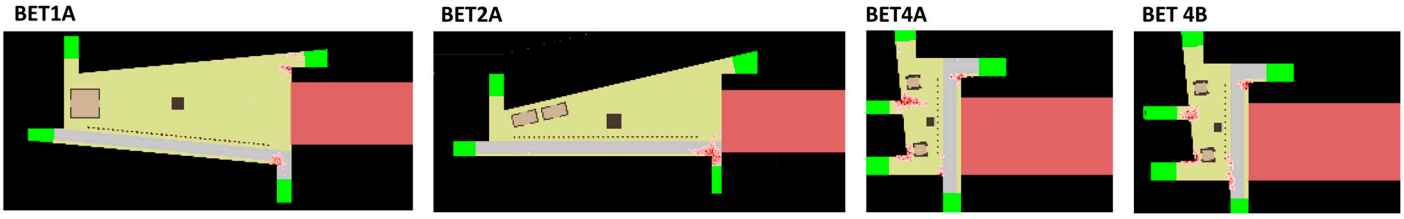

Figure 8. Local analysis of physical contact among the users (maximum probability in dark red) for the analysed BETs. Shown data are similar for all the tested configurations combinations.

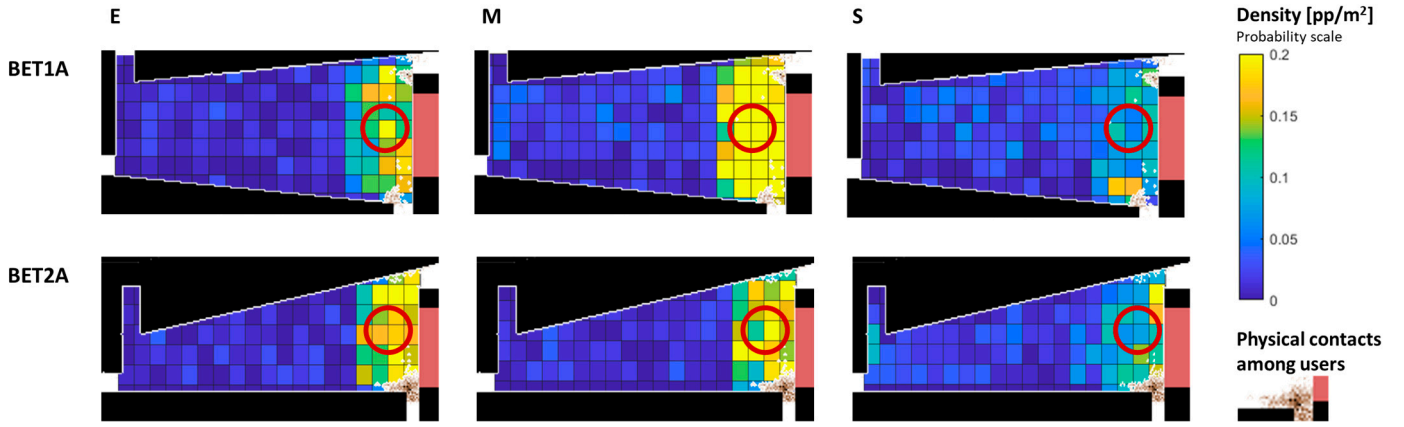

Figure 9. Points of physical contact among the users (higher probability is expressed by dark brown dot colours) and initial users' distribution (in terms of density) for BET1A (first line) and BET2A (second line) for the UTCI-effects scenarios (column). Cells are organized in a 5 m × 5 m grid according to the ENVIMET simulation outputs. The red circle traces the general position area for the attackers. Codes refer to Table 1.

In Figure 6d, the *CR* values for the "no attackers" scenarios are always equal to zero since there are no casualties (compare Sections 3.1.4 and 3.2). The "cold weapon attack" scenarios are characterized by different boxplots depending on the UTCI-effects scenarios, whose vertical extension and median position essentially depend on the possibility of interferences between the prey (the evacuees) and the predators (the attackers), especially at the beginning of the simulation. In fact, at the beginning of the simulation, the initial users' distribution can be more or less dense where the attackers are placed, depending on the BET morphology. In particular, for BET1A and BET2B, the CR results suggest that the risks for users decrease with the increase in the UTCI-effects on the initial users' distribution, while the same phenomenon is not seen for BET4A and BET4B. This result can be essentially connected to the UTCI maps (Figure 3). Figure 9 represents the UTCI effects on the users' distribution for BET1A and BET2A, as expressed by the users' density [pp/m^2], according to the simulation data.

In Figure 9, the users' densities in front of the special building, where the attackers are initially placed (red circle), are higher for the "no effects" and "moderate effects" scenarios than for the "significant effects" scenarios. In fact, when the UTCI effects increase, the users waiting to enter the special building try to move towards the shaded areas that are placed near the built fronts and the access streets (compare with Figure 3), thus reducing

the users' density in front of the special building itself. On the contrary, in the "no effects" scenarios, the density is more homogeneous than in the "moderate effects" scenarios all over the square, since the *PA* is not affected by the UTCI.

As a consequence, these phenomena also impact the *NE* distributions, as shown in Figure 7. In the "no attackers" scenarios, the *NE* is always limited, thus showing that all the users can evacuate the square within the maximum simulation time and that almost none of them prefer to stop inside it (e.g., in a dehors, perceived as a "safe" place in case the access streets are considered as too far—compare with Appendix C). Differences exist in the "cold weapon attack" scenarios, following the same trends as the *CR*.

4.2. Statistical Test Results

Figure 10 presents the results used to investigate if "the climate-related effects on users alter the risk, considering the same morphology and attack scenario" (first research question). For each combination of BET morphology (first column), attack (second column) and UTCI effects (third column), the median values of these indicators (fourth to eighth columns) are presented. Then, the percentage differences in their median values are offered with respect to the "no effects of the UTCI" scenarios (first white line of each combination), in association with their statistical significance (as traced in the legend). In particular, when statistical significance is shown in Figure 10, the percentage differences among the scenarios are relevant because, at least, the calculated *p*-value is smaller than *alpha* = 0.05, and then we should reject the null hypothesis (no difference among the samples). For the conditions with statistical significance, the impacts of the percentage differences are also graphically stressed by colours, considering five main ranges: <−25%, implying a strong reduction in the indicator, thus a significant increase in safety; between −25% and −10%, implying a limited decrease in the indicator; between −10% and +10%, implying similar conditions in the indicator; between +10% and +25%, implying a limited increase in risk indicator; and >25%, implying a significant increase in the users' risk level due to the indicator.

BET	ATTACK	UTCI	TN95	FN95	PN	CR	NE	dTN95	dFN95	dPNp	dCR	dNE
1A	A	E	0.248	0.555	0.198	0.000	0.002					
		M	0.241	0.543	0.170	0.000	0.002	-3% ( )	-2% ( )	-14% (**)	n.a.	-33% ( )
		S	0.247	0.554	0.091	0.000	0.002	0% ( )	0% ( )	-54% (***)	n.a.	-33% ( )
	W	E	0.341	0.702	0.408	0.084	0.083					
		M	0.352	0.701	0.417	0.061	0.061	3% ( )	0% ( )	2% (*)	-27% ( )	-26% ( )
		S	0.343	0.684	0.264	0.038	0.039	1% ( )	-3% ( )	-35% (**)	-55% ( )	-53% ( )
2A	A	E	0.421	0.724	0.452	0.000	0.007					
		M	0.251	0.538	0.242	0.000	0.002	-40% (***)	-26% (***)	-46% (***)	n.a.	-75% (***)
		S	0.364	0.680	0.332	0.000	0.005	-13% (***)	-6% (***)	-27% (**)	n.a.	-25% (**)
	W	E	0.451	0.766	0.491	0.148	0.151					
		M	0.272	0.629	0.260	0.144	0.144	-40% (***)	-18% (***)	-47% (***)	-2% (*)	-4% (*)
		S	0.418	0.743	0.373	0.098	0.103	-7% (**)	-3% (**)	-24% (**)	-34% (*)	-32% (*)
4A	A	E	0.174	0.477	0.207	0.000	0.002					
		M	0.180	0.495	0.202	0.000	0.002	3% (**)	4% (**)	-2% ( )	n.a.	0% ( )
		S	0.194	0.530	0.173	0.000	0.002	11% (***)	11% (***)	-16% ( )	n.a.	0% ( )
	W	E	0.181	0.524	0.213	0.082	0.084					
		M	0.199	0.557	0.244	0.065	0.066	10% ( )	6% ( )	15% (*)	-21% ( )	-21% ( )
		S	0.195	0.566	0.191	0.094	0.096	7% ( )	8% ( )	-10% (**)	14% ( )	15% ( )
4B	A	E	0.174	0.477	0.207	0.000	0.002					
		M	0.178	0.487	0.201	0.000	0.002	2% (**)	2% (**)	-3% ( )	n.a.	0% ( )
		S	0.197	0.538	0.239	0.000	0.002	13% (***)	13% (***)	16% ( )	n.a.	0% ( )
	W	E	0.181	0.524	0.213	0.082	0.084					
		M	0.201	0.577	0.238	0.083	0.084	11% (**)	10% (**)	12% ( )	1% ( )	0% ( )
		S	0.195	0.573	0.156	0.105	0.107	7% (*)	9% (*)	-27% ( )	27% ( )	28% ( )

Legend

Significance:
* = <0.05
** = <0.01
*** = < 0.01 at the general level + <0.05 for the specific combination

Percentage differences for significant combinations:
< -25%
between -25% and -10%
between -10% and + 10%
between +10% and +25%
>+25%

Figure 10. Median values of the key performance indicators for the tested combinations and related calculation of the percentage differences, as compared to the "no effects of the UTCI" scenarios (including statistical significance of the differences). n.a. = not assessed due to computation issues (i.e., the reference indicator is equal to 0). Codes refer to Table 1.

In general terms, the statistical tests denote that the majority of scenarios seem not to come from the same sample, thus underlining that differences due to the UTCI effects exist. Nevertheless, the differences are more relevant in BET2A, which is the widest and least symmetric one, thus confirming the issues concerning the initial users' distribution discussed in Section 4.1 (i.e., Figures 6 and 9). In these cases, the "moderate" and "significant"

UTCI effects seem to generally reduce the risk levels for the users in respect of the "no effects" conditions, especially in the simulations without the attackers, which is as expected (code A in Figure 10). On the contrary, the BET1A differences are not fully supported by the statistical significance tests, while the differences are limited in percentage terms. Moreover, the low increase in the risks due to the UTCI effects in BET4A and BET4B is shown by the *TN95* and *FN95* having statistical relevance. Meanwhile, the effects on the *CR* and *NE* are in this case not relevant in view of the limited open spaces in these BETs, moving towards lower differences in the users' distribution (compare with Figure 3).

Table 2 presents the *p*-values of the Scheirer–Ray–Hare tests used to investigate if "the climate-related effects and morphology alter the risk under the same attack scenario". In this case, the key performance indicators have been aggregated by the terrorist act scenario. According to the calculated *p*-values, differences in all the indicators are noticed due to the BET morphology, which is as expected. In addition, while the UTCI effects by themselves seem not to reach the significance threshold, the combination between the BET morphology and the UTCI-effects scenarios is most of the indicators for both the attack conditions, although they are differently involved depending on the scenario. This phenomenon could be essentially attributed to the initial users' distributions depending on the dimensions of the open spaces, thus following the comments in Section 4.1.

Table 2. Scheirer–Ray–Hare test results for the "no attackers" and "cold weapon attack" conditions. * = significance according to *alpha* = 0.05. (a) = not relevant since the "no attackers" scenarios have no casualties (thus, reporting n.a. values as not assessed).

Attack	Factor	*p*-Value *TN95*	*p*-Value *FN95*	*p*-Value *PN*	*p*-Value *CR* (a)	*p*-Value *NE*
A	BET	<0.01 *	<0.01 *	<0.01 *	n.a.	<0.01 *
	UTCI	0.058	<0.01 *	0.3346	n.a.	0.035 *
	BET × UTCI	0.152	0.004 *	0.004 *	n.a.	<0.01 *
W	BET	<0.01 *	<0.01 *	<0.01 *	<0.01 *	<0.01 *
	UTCI	0.880	0.634	0.166	0.472	0.450
	BET × UTCI	0.028 *	0.024 *	0.001 *	0.104	0.124

The results of the Dunn's tests are reported in Supplementary Material Table S1 to show where differences are mainly noticed. As expected, in both the "no attackers" and "cold weapon attack" scenarios, the null hypothesis of this test should be rejected while comparing the compact BETs (i.e., BET4A and BET4B are in the same layout-based group) and wider BETs (i.e., BET1A; BET2A), especially for the *TN95*, *FN95* and *PN*. This means that differences in the indicators due to morphology could exist. Such a result seems to be extended to the different BET × UTCI effects combinations homogeneously. Nevertheless, the tests fail to reject the null hypotheses while comparing the different UTCI-effects scenarios within this compact morphology, supporting what is discussed in Section 4.1. Dissimilarities between the BET1A and BET2A scenarios could exist for the *PN* and *NE* (and, for the "cold weapon attack" scenarios, also for the *CR*), given the different layout configurations and also considering the same UTCI-effects conditions. On the contrary, the null hypothesis can be accepted for the *TN95* and *FN95* while contrasting BET1A and BET2A for the same UTCI-effects scenarios. The similarities in the square dimensions could have affected this result.

Finally, Figure 11 presents the results used to investigate if "the attack scenario with cold weapons increases users' risks with respect to the conditions without the attackers" (third research question).

Figure 11 is organized according to the scheme of Figure 10. In this case, the percentage differences in the median values of the indicators compare the "cold weapon attack" scenarios with the "no attackers" scenarios (first white line of each combination), in association with their statistical significance (as traced in the legend). In particular, when statistical significance is shown in Figure 11 the percentage differences among the scenarios are relevant

because, at least, the calculated *p*-value is smaller than *alpha* = 0.05, and then we should reject the null hypothesis (no difference among the samples). As expected, the differences between the "cold weapon attack" and "no attackers" scenarios are generally relevant for the *TN95* and *FN95* for all the BETs and all the UTCI-effects conditions. Furthermore, as expected, the risk levels increase, especially in BET1A. The *CR* differences are not relevant since the "no attackers" scenarios have no casualties. The same comment could be linked to the *NE* assessment, as discussed in Figure 7.

BET	UTCI	ATTACK	TN95	FN95	PN	CR	NE	dTN95	dFN95	dPNp	dCR (a)	dNE (a)
1A	E	A	0.248	0.555	0.198	0.000	0.002					
		W	0.341	0.702	0.408	0.084	0.083	38% (**)	26% (**)	106% (**)	n.a.	3361% (**)
	M	A	0.241	0.543	0.170	0.000	0.002					
		W	0.352	0.701	0.417	0.061	0.061	46% (**)	29% (**)	145% (**)	n.a.	3717% (**)
	S	A	0.247	0.554	0.091	0.000	0.002					
		W	0.343	0.684	0.264	0.038	0.039	39% (**)	24% (**)	189% (**)	n.a.	2328% (**)
2A	E	A	0.421	0.724	0.452	0.000	0.007					
		W	0.451	0.766	0.491	0.148	0.151	7% ( )	6% (**)	9% ( )	n.a.	2196% (**)
	M	A	0.251	0.538	0.242	0.000	0.002					
		W	0.272	0.629	0.260	0.144	0.144	8% (**)	17% (**)	7% ( )	n.a.	8648% (**)
	S	A	0.364	0.680	0.332	0.000	0.005					
		W	0.418	0.743	0.373	0.098	0.103	15% (*)	9% (**)	12% ( )	n.a.	1986% (**)
4A	E	A	0.174	0.477	0.207	0.000	0.002					
		W	0.181	0.524	0.213	0.082	0.084	4% (*)	10% (**)	3% ( )	n.a.	4958% (**)
	M	A	0.180	0.495	0.202	0.000	0.002					
		W	0.199	0.557	0.244	0.065	0.066	10% (**)	13% (**)	21% (*)	n.a.	3892% (**)
	S	A	0.194	0.530	0.173	0.000	0.002					
		W	0.195	0.566	0.191	0.094	0.096	1% ( )	7% (*)	10% ( )	n.a.	5705% (**)
4B	E	A	0.174	0.477	0.207	0.000	0.002					
		W	0.181	0.524	0.213	0.082	0.084	4% (*)	10% (**)	3% ( )	n.a.	4958% (**)
	M	A	0.178	0.487	0.201	0.000	0.002					
		W	0.201	0.577	0.238	0.083	0.084	13% (**)	18% (**)	18% ( )	n.a.	4966% (**)
	S	A	0.197	0.538	0.239	0.000	0.002					
		W	0.195	0.573	0.156	0.105	0.107	-1% ( )	6% (**)	-35% ( )	n.a.	6372% (**)

Legend

Significance:
* = <0.05
** = <0.01

Percentage differences for significant combinations:
< -25%
between -25% and -10%
between -10% and + 10%
between +10% and +25%
>+25%

Figure 11. Median values of the key performance indicators outlined for the tested combinations and the related calculation of the percentage differences, as compared to the "no attackers" scenarios (including statistical significance of the differences). "n.a." = not assessed due to computation issues (i.e., the reference indicator is equal to 0). (a) = not relevant since the "no attackers" scenarios have no casualties. Codes refer to Table 1.

5. Discussion

5.1. Simulation Insights in View of the Research Questions

Thanks to the adopted simulation-based approach, this work verifies that taking into account (or not) the effects of the outdoor temperature on the initial users' distribution in public open spaces (squares) can alter the risk for them in case of a terrorist act.

Three experimental-based square archetypes, representing recurrent square morphologies, are considered for the evacuation simulation in public open spaces due to the "no attack" and "cold weapon attack" scenarios [48]. Simulations of the outdoor temperatures are performed using ENVIMET to report the UTCI values, and three critical increasing temperature scenarios are selected thanks to a previous work's results [30]. Then, this work considers the "no effects of the UTCI" scenario (as in normal comfort conditions of users placed outdoors) and "moderate" and "significant effects of the UTCI" on users' distribution in public open spaces (which can hence represent two behavioural responses to increasing temperature conditions) [29]. Experimental-based typological conditions relating to the users' exposure and vulnerability are also included as simulation inputs [9].

In particular, considering the three main research questions expressed in the work aims (Section 1.1), the simulation results and their statistical analysis suggest what follows.

1. "Do the climate-related effects on users alter the risk, considering the same morphology and attack scenario?" Yes, the climate-related effects on users alter the risks when the users majorly react to the increasing temperature scenarios under the following specific morphology and attack conditions:
    - In the widest and less regular square archetype (i.e., BET2A), in both attack scenarios, all the considered indicators decrease (up to about −50%) because a

more widespread distribution of users is ensured and fewer interferences with other users and the attackers (when present) are noticed during the evacuation movement. In fact, while looking for shaded areas nearby the built fronts, the users are thus placed in lower crowding conditions, and they increase their distance from the attack source.

- On the contrary, the risks connected to the evacuation timing (*TN95*) and flows (*FN95*) slightly increase (up to about +15%) for the most compact and regular BETs (BET4A and BET4B). Local crowding conditions can increase in view of the higher number of users in shaded areas, causing a slight reduction in the evacuation speediness, although the effects are less relevant in view of the reduced spaces dimensions.

2. "Do the climate-related effects and morphology alter the risk under the same attack scenario?" Yes, as a further consequence of point 1, the combination of climate-related effects and morphology alters the users' risk under the following specific attack scenario:
   - The combination of the UTCI effects and morphology is significant for the evacuation timing (*TN95*) and flows (*FN95*), as well as for the physical interactions among users (*PN*), especially when attackers are present. As expected, the risks are higher in the widest and most complex square (i.e., BET2A) in view of comments in relation to point 1.
   - Moreover, as expected, the BET morphology is a significant factor by itself. The higher the open space dimensions and irregularity in shapes, the higher the *TN95* and *FN95*. The *PN* increases in less regular scenarios (i.e., BET2A). The *CR* is lower in wider and regular open spaces (i.e., BET1A).
3. "Does the attack scenario with cold weapons increase users' risks with respect to the conditions without the attackers?" Yes, the attack scenario with cold weapons increases the users' risks with respect to the conditions without the attackers in all the BETs and for all the UTCI-effects scenarios, which is as expected. Although the riskiest scenarios in absolute terms occur in the widest and most complex square archetype (BET 2A), a higher increase in the risks (up to about +50% for *TN95* and +200% in *PN*) is noticed for the wide but regular square (i.e., BET1A). This result demonstrates that the significant alterations in the risks are due to the prey–predator logic of the attackers, which can disturb the evacuation movement in a significant manner even though the built environment has a simple layout configuration.

5.2. Limitations and Future Works

The assessed scenarios are typological representations and rely on the recurrent, cluster-based, archetype-based conditions of historical Italian squares in terms of the hazards (i.e., soft-target presence and terrorist act typology), morphology, climate scenarios, and users' exposure and vulnerability. In detail, the tested BET morphologies are representative of a wide sample of Italian squares (Section 3.1) [48]. The outdoor increasing temperature scenarios are derived from validated works in the considered climate context and the BETs [30]. The users' reactions to thermal stress in increasing temperature conditions are derived from experimental-based correlations [29]. The users' exposure and vulnerability scenarios are derived from real-world case studies in the Italian context [9]. The possibility of a terrorist act in a square is supported by its typical characterization as a soft target because of its use at the national and international levels [16,18,19,22]. In this sense, this contribution hence succeeds in defining a methodology for risk assessment according to simulation modelling and analysis based on the proposed key performance indicators. At the same time, it demonstrates that differences due to the input factors exist (Section 5.1).

Nevertheless, the authors are aware that this contribution can represent a preliminary work towards more wide analyses of the mutual influence of the tested factors. In fact, the number of simulated combinations is still limited. Further input scenarios should be hence

considered in subsequent research steps. To this end, previous works on the BETs characterization could be used as priority references to enlarge the simulation scenarios [48,59,61]. Such simulations will aim at highlighting if differences due to such risk factors exist among other "idealized" built environment conditions.

It is also worth noting that the simulations are just focused on a single open space in the urban built environment, thus simplifying the correlation with the surrounding urban fabric. This choice is functional to the specific assessment of the square risks, which is the core of our research. Furthermore, this perspective is consistent with the evacuation criteria in squares, which imply a quick exit of the attacked outdoor area by allowing users to move towards the surrounding street network [3,25]. Nevertheless, future efforts could aim at placing the assessed squares into a typological urban fabric to evaluate the additional effects of the urban form in normal use (i.e., users' flows entering or leaving the square) and evacuation (including other emergencies, e.g., earthquakes) [10].

Additional climate conditions to derive the UTCI values in the BETs should be tested by preliminarily focusing on the built fronts heights in respect of the open space dimension [15]. Concerning the increasing temperature conditions, no risk mitigation strategies have been tested in this work. Thus, future studies should implement heat stress mitigation solutions, such as shadings, trees and cooling surfaces implementation, that will affect the initial user generation in public open spaces depending on behavioural issues and thermal acceptability [14,29,31,32]. At the same time, additional efforts to simulate the individual features affecting the thermal response and stress could be included, thus improving the acceptability algorithm and making it "tailored" to different scenario conditions. Issues concerning the collective attitudes of users and their mutual interaction could be implemented to create "groups" of users, also depending on a more detailed definition of their activities (e.g., touristic, market experience, merely passing through the open spaces, participating in outdoor recreation tasks) [14].

The simulations are essentially based on typological users' exposure and vulnerability issues, and thus further crowding levels could be tested, starting from statistical-based ones derived from real-world historical squares analysis [9].

Several attack typologies can be investigated within each BET by using this work's simulation-based approach. For instance, apart from the adopted basic prey–predator logic for the attack, a combination of cold weapons and exploding handcrafts (e.g., backpacks or easily concealable fanny packs with small pipe bombs) could be included in the simulation scenarios to include conditions in which the attackers would like to drive the public into the arms of the terrorists waiting with cold weapons. Furthermore, other scenarios will concern attacks with other kinds of weapons (including shooters' attacks), bombing, and a vehicle running into the crowd [19]. In this sense, multiple or combined terrorist act sources could be also considered in the public open space, as well as different localizations within the square depending on the soft target position [9,14,18]. For instance, it could be possible to move towards simulations by considering, e.g., (a) two attackers generated in different positions, (b) whether the attackers can have (or not) any plan/hope of escaping after the attack, (c) that the attack can start inside a special building or at its entrance, or (d) that the attackers would move towards the crowds to drive them towards a specific part of the open spaces. Variations in the terrorism self-aid procedure probability threshold could also describe the effectiveness of the attack (or of countermeasures, including the presence of police and other first responders), as well as the agility and abilities of the attackers or of the evacuees [36,57,81,85].

From a modelling perspective, the affordance-based parameters affecting the users' motion, as shown in Section 2.2, could indeed be modified. The dynamic floor field, which is currently calculated according to the Priority Queue Flood Fill Algorithm, could be substituted by other approaches to provide different evacuation paths (e.g., A*). Such modifications could be able to represent different excitement levels of the crowd and their preferences in moving towards/avoiding areas, attackers, obstacles and other users [43,58,87,93,94]. This work does not consider differences in premovement times, instead focusing on the critical

densities of users moving contemporarily (Section 3.2). This choice also allows us to reduce uncertainties due to behavioural effects at the simulation start and to focus on the effects of the local outdoor temperature on users' distribution. Therefore, additional users' reaction levels, depending on the attack source, could be added in further works, including both premovement times, additional uncertainties in evacuation path selection and fighting behaviours [23,37,38,44,47,58]. For instance, visual and sound stimuli (e.g., the view of the attackers, of their weapons, and of running crowds; hearing screaming of other users or the sound of the attack) and their combination could be added to the model, also considering the distance from the attack source and where the attention of the users is focused before the evacuation process (e.g., mass gatherings, marketplaces, presence of stages in the square). Visual features and acoustic dynamics of/in the open space could be then considered in such cases to include issues concerning morphology and construction technologies. Nevertheless, the use of agent-based modelling and cellular automata could be flexible enough to support future integrations and modifications by using the same general modelling approach as this work [43,87,90,94].

This work relies on the use of typological scenarios rather than specific case studies to outline the general issues that can affect samples of squares connected to the tested archetype [42,43,49]. Further efforts have to hence be devoted to the comparison of risk performances in typological versus real-world built environments, starting from squares sharing the same features as the selected archetypes. The same simulation-based approach could be used. Such a task will represent a useful step towards "tailoring" strategies depending on the specificities of each real square. These research outcomes could support local authorities and their technicians when performing a quick preliminary risk assessment of the public open spaces in historical urban built environments.

The simulation-based approach and comparison perspective can be then employed to evaluate how mitigation interventions comprising architecturally integrated solutions (including wayfinding strategies) could affect the risk for users. This work tests a unique common internal layout for all the BETs (poles along the carriageway and central monument). Thus, the re-organization of outdoor spaces could hence be a key leading strategy to mitigate the risk of terrorist acts in the investigated BETs by supporting the evacuation of users [19,20,22]. These interventions can decrease the probability of specific attacks (e.g., internal architecture and fixed obstacles can reduce the occurrence and the effects of attacks with vehicles running into the crowd) [22]. Nevertheless, these choices should guarantee free access for pedestrians, and they should not represent obstacles to evacuation from the square. Furthermore, practical and aesthetic purposes can be used to implement such barriers in view of the whole value of the tangible cultural heritage represented by the historical squares, the urban context where they are placed, and the hosted artefacts [1]. In addition, risk management solutions should be included in the event modelling, such as those based on the presence of safety and security staff members who can prevent attackers from directly entering the most crowded area or who can support the evacuees and react towards the attackers [81]. These kinds of activities will allow the ranking of safety depending on the squares' features and on the risk mitigation solutions implemented. As a result, a preliminary analysis of the best strategies in each BET could be proposed, also depending on the specific attack conditions.

Finally, the provided key performance indicators are herein not linked together but represent different issues in relation to the risk for the users placed in the square (i.e., outdoors). Metrics should be developed to combine them and to obtain a unique risk value for each of the tested conditions.

6. Conclusions and Remarks

The historical urban built environment is a complex system composed of tangible cultural heritage, buildings, urban infrastructure, public open spaces and users. In this overall context, historical squares are fundamental elements because of their morphology in respect of the surrounding complex and narrow urban fabric and for their attractive effects

on users, over time and space, due to the hosted tangible cultural heritage and related sights. For these reasons, the protection of the cultural heritage against disasters should be founded on risk assessment tasks and should take into account the squares as paramount scenarios for increasing the safety of the whole historical city and its hosted population. Nevertheless, such a task should rely on the development of quick but reliable risk assessment methods, which can also investigate how boundary scenario conditions can alter the risk for squares' users. In this sense, users' behaviours in response to increasing temperature scenarios are one of the most critical factors to be assessed in view of climate-change issues.

This work represents one of the first attempts to investigate how the risks in public historical squares can change depending on users' behaviours in response to the outdoor (increasing) temperature and evacuation due to terrorist acts. In this sense, it also represents a basic step towards the proposal and assessment of mitigation strategies in combination with heritage preservation criteria in the context of emergency scenarios. In particular, the approach will contribute to the evaluation of current and mitigated conditions in view of heritage preservation tasks, which could be better carried out by considering their effective impacts not only on the heritage but also on the users.

In this general context, the research also inspects differences in the users' risks depending on the squares' morphology and on the attack source. To this end, a simulation-based approach is developed and then preliminary verifications and capability demonstrations are shown for some selected Built Environment Typologies (BETs) representing archetypes of historical squares in the Italian context. Therefore, the effects of the squares' morphology have been also considered by modelling different kinds of squares relying on their basic typological features. This work uses increasing temperature conditions to influence the initial users' distribution in public open spaces. Different users' behaviours in view of the thermal acceptability have been considered: the first one simulates that the users are always in comfort conditions and thus there is no influence of the outdoor temperature on the initial users' distribution in the public open space; in the second and the third cases, the UTCI effects on the users' response increase gradually. Then, the evacuation process from the square is considered in view of a possible terrorist attack with cold weapons. Combinations of morphology, climate effects and attack configurations are organized, using the same users' exposure and vulnerability scenario as a constant input. The simulation results are assessed by using key performance indicators representing different behavioural issues in the evacuation.

The results demonstrate that increasing temperature scenarios can affect the users' risk by generally decreasing it in wide and complex BETs and increasing it in compact and regular BETs. At a glance, such an effect is essentially due to the impact of the users' distribution and the related crowding levels while looking for shaded areas where they can be protected from high temperatures, which is as expected. The use of typological conditions has been considered since the idealized open spaces simulated in this work represent archetypes of real-world squares and, in such a way, can provide general insights for specific case studies. In this sense, this contribution also represents a further step in the BE S^2ECURe project, of which this work is part. In view of a general ranking of the BETs among the risks, we can also conclude that local administrations and safety planners should pay particular attention to the design of risk strategies in wide but complex squares.

The next steps will concern the application to real-world squares, since this work provides general results at the broadest level, that is, using archetypes of squares, and thus it may be informative for stakeholders. The application to real-world squares can contrast and compare this work's outcomes to confirm (or not) the provided KPI trends or give further details due to the specificities of real-world contexts with respect to idealized ones. In fact, the authors would like to acknowledge that every urban square is different in terms of the morphology (i.e., spatial layout and overall size), vehicular access (general or during specific hours), internal architecture and obstacles placed in open spaces (e.g., fountains, presence of cafés and dehors, at the margins or in the centre of it, nature of access points) and, finally, usage and users' movement flow by people (residents and tourists).

The proposed simulation model follows an experimental-based microscopic approach to the users' behaviours, using quick-to-apply simulation techniques in terms of the square description and computation time. At the same time, it can reliably represent individual choices in disaster-stricken scenarios. The whole method also provides simple risk indicators relying on previous behavioural design literature works, which can be used to compare the risk levels in different scenario conditions.

Although the application is herein limited to terrorist acts, the same approach can be used for any emergency conditions that have a strong relationship with the built environment features and the hosted users. Other boundary environmental conditions that affect the users' distribution in the square could be selected and modelled according to the same approach. For instance, the air pollutant concentration in open spaces could be modelled depending on the presence of pollutant sources. The users' perception of the environmental quality can change and imply different uses of the open spaces themselves to avoid direct exposure to critical scenarios. Similarly, other accidents that imply emergency response and evacuation from or towards the square could be included too. For instance, earthquake evacuation towards the square could be modelled by adapting the proposed general motion rules. Specific setups will consider the generation of users depending on the input drivers, the affordance-based path selection, the motion speed and the fundamental diagram of pedestrian dynamic to make to scenario consistent with experimental assumptions.

Finally, this work is focused on risk assessment and does not refer to risk mitigation. Nonetheless, the provided results suggest that decision-makers could take advantage of the proposed approach and simulation tool, moving towards the analysis of how the implementation of mitigation solutions to increase the thermal comfort for users can affect the risk levels in an evacuation. Similarly, strategies for evacuation support could be tested by verifying the combination of impacts with respect to increasing temperature scenarios.

Supplementary Materials: The following supporting information can be downloaded at https://www.mdpi.com/article/10.3390/heritage6070274/s1, Table S1: Dunn's test results for the "no attackers" and "cold weapons attack" scenarios (csv file).

Author Contributions: Conceptualization, G.B, E.Q. and M.D.; methodology, G.B., E.Q. and M.D.; software, G.B.; validation, G.B. and E.Q.; formal analysis, G.B.; resources, E.Q.; data curation, G.B.; investigation, G.B. and E.Q.; writing—original draft preparation, G.B.; writing—review and editing, E.Q. and M.D. visualization, G.B.; supervision, E.Q. and M.D.; project administration, E.Q.; funding acquisition, E.Q. All authors have read and agreed to the published version of the manuscript.

Funding: This research was funded by the MIUR (the Italian Ministry of Education, University, and Research) Project BE S^2ECURe—(make) Built Environment Safer in Slow and Emergency Conditions through behavioUral assessed/designed Resilient solutions (grant number: 2017LR75XK).

Data Availability Statement: The data presented in this study concerning the POS characterization in the BETs and the simulation model are available online on the website of the BE S^2ECURe project: https://en.bes2ecure.net/ https://en.bes2ecure.net/wp3 https://en.bes2ecure.net/wp4 (accessed on 25 June 2023). Extended simulation data are available from the corresponding author, G.B., upon reasonable request.

Acknowledgments: The authors would thank Dr. Valeria De Matteis for her support in performing the simulation.

Conflicts of Interest: The authors declare no conflict of interest.

Appendix A. Main Notations and Acronyms

Table A1. Main notations and acronyms, in alphabetical order. Unit of measurement: "-" is used for a non-dimensional parameter.

Notation/Acronym	Definition	Unit of Measure (If Appliable)
$Aff_{c,}$	Affordance of a given cell, at a given time in the simulation; see Appendix C	-
BET	Built environment typology	
c	Index of the cell in the simulation environment	x, y coordinates
CR	Casualty ratio	-
$F_{d,c,t}$	Distance from a given cell to the closest safe area in the BET; see Appendix C	data
$F95$	Flows at the evacuation targets based on the analysis of 95% of the users so as to avoid considering effects due to "outlier" model uncertainties	pp/s
$FN95$	Normalized flows; see Equation (2)	-
i	Index of the simulated user	
k	Shaping coefficient in the fundamental diagram of the evacuation speed; see Appendix C	-
NE	Median number of users who did not complete the evacuation during the simulation time	pp
$O_{c,t}$	Distance of the cell c from buildings and monuments	-
$P_{c,t}$	Pedestrian density "near" a given cell placed near a user, at a given time; see Appendix C	-
PA, PAh, PAt	Probability of UTCI-based acceptability, probability of dehors, and probability of pedestrian areas; see Equation (1)	%
PCF	Relative number of physical contacts among users and falls, as obtained by dividing the number of contacts and falls by $T95$	events/s
PN	Normalized number of physical contacts among users; see Equation (3)	-
$R_{c,t}$	Risk in a given cell of the open space due to the considered terrorist attack	-
t	Index of time in the simulation	s
$T95$	Evacuation time based on the analysis of 95% of the users so as to avoid considering effects due to "outlier" model uncertainties	s
$TN95$	Normalized evacuation time, equal to the ratio between the $T95$ and the maximum simulation time (i.e., in this work 150 s)	-
UTCI	Universal Thermal Climate Index	°C
Vi	Users' evacuation speed; see Appendix C	m/s
V_{max}	Maximum evacuation speed of the user, that is, in free-flow motion conditions (null density); see Appendix C	m/s
V_{min}	Minimum evacuation speed of the user, that is, in at maximum experimental density ρ_{max}; see Appendix C	m/s
α	$P_{c,t}$ weight; see Appendix C	-
β	$F_{d,c,t}$ weight; see Appendix C	-
γ	$R_{c,t}$ weight; see Appendix C	-
δ	$O_{c,t}$ weight; see Appendix C	-
ρ_{max}	Maximum experimental density; see Appendix C	pp/m^2

Appendix B. Calculation of Users' Exposure

The calculation of the number of exposed users is based on the experimental-based median values [9] of: (a) the overall outdoor users' density [pp/m^2], (b) the users' density with respect to the special building [pp/m^2], and (c) the percentage of users placed outdoors. These values have been calculated in reference to the widest square, that is, the one of BET1A, to maximize the number of exposed users. Equation (A1) presents the complete calculation of the number of exposed users.

$$exposed\ users = \left[\left(0.2\ pp/m^2 * 3000\ m^2\right) * 24\%\right] + \left[0.4\ pp/m^2 * 1200\ m^2\right] \approx 625\ pp \quad \text{(A1)}$$

The median overall outdoor users' density is considered as equal to 0.2 pp/m^2 [9]. Then, this value is multiplied by the BET1A outdoor area so as to obtain the overall number of users who populate the BET both indoors and outdoors. The percentage of users placed outdoors is equal to 24% [9], which should be multiplied by the overall number of users. These outdoor users are: (a) passersby (23%), who are generated in the pedestrian areas; and (b) users placed in dehors (1%). The users of the special building in the BET, which is assumed as a church, are generated in front of it to consider that they are involved in leisure or social tasks, waiting to enter and visit the special building, or waiting for the religious functions [9,14]. This choice relies on a conservative approach to the terrorist act analysis since it maximises the number of exposed users who can be directly affected by the attack while being placed outdoors. This value has been calculated as the multiplication between the median users' density for special buildings open to the public (i.e., 0.4 pp/m^2) and the median surface of the special buildings, that is, 1200 m^2 in each BET [9]. Thus, an additional 480 users are obtained. The final number of users is then equal to 625 pp.

Appendix C. Evacuation Model Description

The simulation assumptions are consistent with previous approaches to terrorist act evacuation [36–38,47,57,83], mainly with those adopting cellular automata [38,44] and agent-based modelling [36,37,82–85].

To simulate the *users'* movement, an affordance-based criteria approach [43] is adopted to create a dynamic floor field that can "describe the willingness to walk" of a user placed in a certain cell towards one of the evacuation targets [87]. This approach considers that, at a given time t, each cell c has a given affordance $Aff_{c,t}$ [-], as shown in Equation (A2). The higher the $Aff_{c,t}$, the higher the probability that the user can select c.

$$Aff_{c,t} = \alpha P_{i,c,t} + \beta F_{d,c,t} + \gamma R_{c,t} + \delta O_{c,t} \quad \text{(A2)}$$

The $Aff_{c,t}$ is based on four factors, which are evaluated at each simulation step t and for each cell c. To ensure a scale comparison, each factor $f_{c,t}$ affecting the $Aff_{c,t}$ ranges from 0 to 1 thanks to the normalization logic of Equation (A3):

$$f_{c,t} = (f_{c,t,max} - f_{c,t}) / (f_{c,t,max} - f_{c,t,min}) \quad \text{(A3)}$$

where the subscripts *max* and *min* refer to the maximum and minimum conditions of the specific factor among the cells.

The $P_{c,t}$ [-] represents the pedestrian density "near" the cell c occupied by the user i according to the extended Moore neighbourhood approach [93]. According to this approach, the reference neighbouring cells are the ones that can be reached by the user with a certain current speed and within a reaction time of 1 s. The cells described as obstacles are excluded. $P_{c,t}$ hence varies over the simulation time depending on the evacuation process.

The $F_{d,c,t}$ [-] concerns the distance from cell c to the closest evacuation target in the BET. According to previous simulation approaches [94], the Priority Queue Flood Fill Algorithm is used to calculate the $F_{d,c,t}$, ensuring a simple but reliable, consolidated and fast approach in the evacuation simulation. In case the safe area is not visible from c because of an obstacle (i.e., buildings, monuments), the distance is increased by a visibility factor, which is assumed to be equal to 4 in our simulations. The $F_{d,c,t}$ does not change over the simulation time and ranges from 0 (most distant cells from the evacuation target) to 1 (closest ones). Figure A1A shows an example of the $F_{d,c,t}$ fields in the context of BET2A.

The $R_{c,t}$ [-] concerns the risk in a given cell c of the open space due to the attack. The $R_{c,t}$ assumes a minimum value in the cells in the attack area, while the $R_{c,t}$ increases with the distance from the attack area. Therefore, the simulation scenarios with no attackers do not include casualties and all the outdoor cells have $R_{c,t}$ = 1.

Meanwhile, in the cold weapon attack scenarios, the $R_{c,t}$ depends on the distance between the attackers and the outdoor cells so as to create a sort of repulsive floor field [47,57,83]. Figure A1B shows the area where the attackers are initially placed at the beginning of the accident (orange circle) for BET2A, as a significant example. This area is here graphically overlapped with the $R_{c,t}$ values for the outdoor cells at the start of the cold weapon attack, that is, at t = 0 s. Herein, the light blue cells refer to the maximum $R_{c,t}$ (close to the attackers' position), while the dark blue cells refer to the minimum $R_{c,t}$. At the simulation start, two attackers are generated in front of the special building, where users waiting to enter it are placed (orange circle in Figure A1B). They start moving in the crowd, according to a typical prey (the evacuees)–predator (the attackers) model [47,57,83], where the prey are the nearest pedestrians to the attacker and then the attacker chases them up to the end of the evacuation process. The attackers are assumed to move independently while chasing the evacuees. An attack range between the attacker and the evacuee [36–38] of 1 m radius is assumed as the threshold for casualties. Nevertheless, the proposed model also considers the probability that a user can be wounded [57], which is associated with the terrorism self-aid procedure (TSAP) probability threshold [%]. A similar approach has been considered also for other disasters implying evacuation (e.g., earthquakes [95]). The users who are not wounded can evacuate, while the others are conservatively assumed as casualties. In this work, the TSAP is conservatively assumed to be equal to 50%. To focus on the users' safety assessment in the evacuation, and considering real-world users' responses and recommendations from law enforcement agencies [23,36], no fighting behaviours are considered in the simulations.

The $O_{c,t}$ [-] represents the distance of the cell c from buildings and monuments and is introduced to consider that each user can limit physical contact with them, according to an interaction distance of 3 m as the literature reference threshold [96].

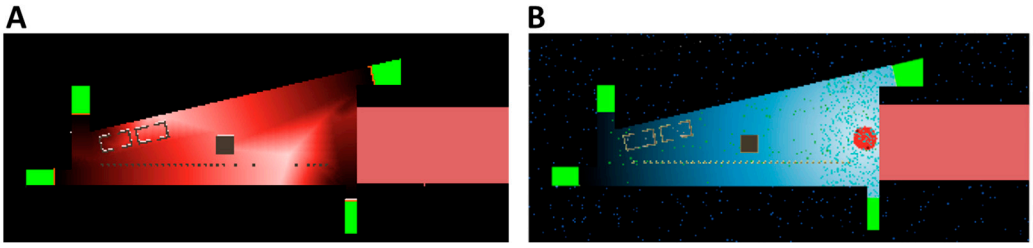

Figure A1. Example schemes for BET2A of (**A**) the $F_{d,c,t}$ (which is the same regardless of the terrorist act) and (**B**) the *Rc,t* maps for the cold weapons attack in front of the church (initial attackers' position inside the orange circle). The $F_{d,c,t}$ ranges from 0 in light red to 1 in dark red. Panel (**B**) shows the *Rc,t* map at t = 0 s. In panel (**B**), the users are blue points, while the *Rc,t* ranges from 0 (maximum risk, in light blue) to ≈1 (minimum risk, in dark blue).

The impact of each factor in Equation (A2) depends on a related non-dimensional weight α, β, γ, δ. The sum of these weights is always 1 [43]. In particular, in the "no attackers" simulations, $\alpha = 0$, $\beta = 1$, $\gamma = 0$, $\delta = 0$ since no additional risks for the users are considered. This setup corresponds to a typical shortest path selection [43,93]. Indeed, the simulations for the cold weapons attacks assume $\alpha = 0$, $\beta = 0.9$, $\gamma = 0.1$, $\delta = 0$ to combine the attraction to the access streets (see β) and the attackers' effects on the users' path choices (see γ).

The evacuation speed for each *user Vi* [m/s] is calculated according to the adaptation of the fundamental diagram for pedestrian dynamics [91] based on experimental values concerning terrorist acts [23], as shown in Equation (A4):

$$Vi = \begin{cases} (V_{max} - V_{min}) * \left(1 - e^{k*(\frac{1}{\rho} - \frac{1}{\rho_{max}})}\right) + V_{min} \; for \; \rho \leq \rho_{max} \\ \max(0, k_L * (\rho - \rho_{max}) + V_{min}) \; for \; \rho > \rho_{max} \end{cases} \quad \text{(A4)}$$

where V_{max} = 2.5 m/s, V_{min} = 0.72 m/s, $k = -0.14$, and ρ_{max} = 2.67 pp/m^2. The linear regression coefficient k_L is applied between ρ_{max} pp/m^2 (for which $Vi = V_{min}$ = 0.72 m/s) and the critical density that can cause an evacuation stop ($\geq$4 pp/m^2) [58]. Thus, the k_L is calculated to linearly interpolate the respective *Vi* values of 0.72 m/s and 0 m/s. The ρ value is calculated according to the abovementioned extended Moore neighbourhood approach [93], albeit by considering only the cells along its movement direction and placed inside their horizontal field of view, which hence represents its visual perception domain [44,96–98] (in this work, equal to about 200°—https://bit.ly/3AYaCIY, accessed on 25 June 2023). The introduction of this sort of visual perception domain also avoids users' sudden movements in direction selection and thus more smoothed users' trajectories.

According to previous works [23,88], the *Vi* is associated with a normal probability distribution, having a standard deviation of 0.7 m/s (which also allows the model to stochastically include the effects of ground slopes), while an age-dependent adjustment of speed is calculated by multiplying the *Vi* by: for toddlers, 0.53; for parent-assisted children, 0.87; for young people, 1.00; for adults, 0.87; and for the elderly, 0.67.

Due to the temporal discretization in the cellular automata approach [87], each simulation step just represents a part of the movement per second, and its time length depends on the maximum evacuation speed for the whole simulated *user* sample. The *users* characterized by the overall maximum evacuation speed move at each tick, while the *users* with lower speeds wait for some time ticks depending on this ratio. The *users* can move one cell between the neighbouring ones, considering those that are placed along its movement direction and inside their horizontal field of view. Asynchronous update rules are considered by randomly selecting the order of pedestrian movements [87]. In detail, the *user* tries to move towards the next free-of-users and -obstacles cells with the maximum $Aff_{c,t}$. However, if the cell is not available, the *user* chooses another cell according to the following order: (a) maximization of the $R_{c,t}$, by selecting cells with a higher $F_{d,c,t}$ to reduce terrorist acts effects; or (b) maximization of the $F_{d,c,t}$, to move towards a safe area; or (c) maximization of the $F_{p,c,t}$, to avoid crowding-related risks; or (d) just selecting one of the other available patches; or (e) otherwise (i.e., in case of congested crowd conditions), the *user* does not move.

To consider additional local conditions during the evacuation [58,96], the *user* can also temporarily stop moving if: (a) the neighbouring pedestrian density is >4 pp/m^2 (compare with the Equation (A4) rules); or (b) the user's evacuation speed reduces suddenly (more than 0.3 g of acceleration between two consecutive time ticks); or (c) the user is moving in a counterflow. Such conditions imply that the *user* can be affected by physical contact and fall to the ground. A probability threshold to stop the evacuation (equal to 5%) is compared by a user's random number [58]. In case the random number is lower than the probability threshold, the *user* waits up to about 30 s, according to a random uniform distribution [58].

Appendix D. Preliminary Verification Results of the Evacuation Simulation Model

The basic scenarios generally used for evacuation simulation validation are used for the preliminary verifications of the proposed model [86]. In particular, a 40 m long straight-line path (based on IMO test 1) is used to verify if the model can represent both isolated users' motion conditions and grouped motion. The path length is consistent also with the typological scenario morphology [48]. Tests are conducted considering the *Vi* equal to 1 m/s as the standard adult non-emergency speed [86], 2.5 m/s as the reference speed for terrorist act evacuation, and according to Equation (A4) [23].

Then, a corner scenario (based on IMO test 6) is used to assess the possibility of navigation of a group of 20 pedestrians without penetrating the BET boundaries considered as obstacles and to compare the outcomes of different values for the weights in the $Aff_{c,t}$ calculation (see Equation (A2)) on the selected paths and evacuation times. The second part of the corner path has a width of about 6 m, which is consistent with the dimensions of the access streets characterizing the assessed typological historical square [48] (compare

with Section 3). In each test, 10 consecutive runs of setup scenarios are performed to keep in mind modelling uncertainties [86].

As expected, the isolated users' motion test along a straight-line path is successfully achieved, obtaining an evacuation time of 40 s for the standard adult walking speed and about 16 s for the terrorist act evacuation speed. The isolated users' trajectories refer to linear cell selections in both the test setups. Then, Figure A2 overlaps the fundamental diagram of the pedestrian dynamics for the terrorist act in Equation (A4) and the density–speed pairs in the grouped users' motion simulation. The simulation model is reliable in describing the density effects, having a mean error <5% of prediction with respect to the fundamental diagram. The same error has been also noticed in the BET-related simulations. The corner scenario tests verify that the users do not penetrate the obstacles and that differences in the path distribution exist depending on the values of the factor weights in Equation (A4). When $\beta = 1$, the users minimize the evacuation path length, also moving nearby obstacles and buildings (Figure A3A). When the factors relying on the obstacle effects are also considered ($\delta > 0$, as in Figure A3B), the paths are more concentrated far from obstacles. When the factors relying on the users' density are additionally included ($\alpha > 0$, as in Figure A3C), the paths are more dispersed since the users try to avoid crowded areas. The positive preliminary verification of the simulation model encourages its application in complex scenarios.

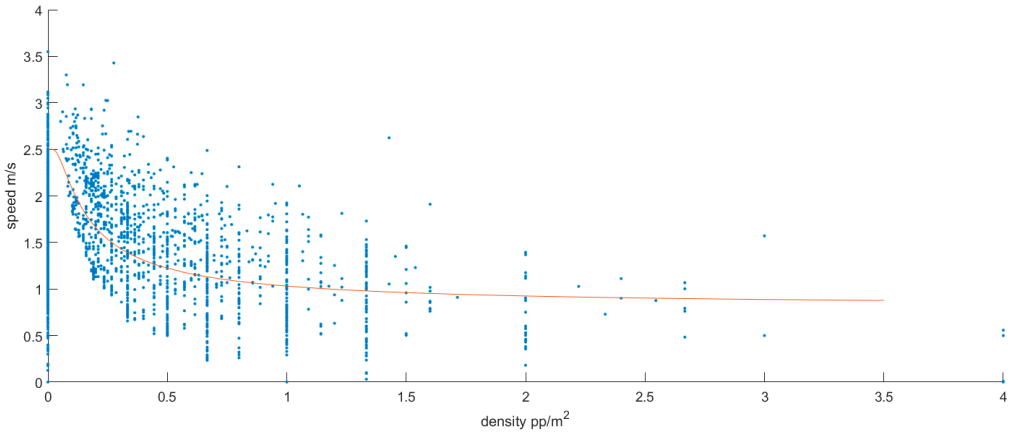

Figure A2. Grouped users' motion tests: overlapping fundamental diagrams with experimental pairs.

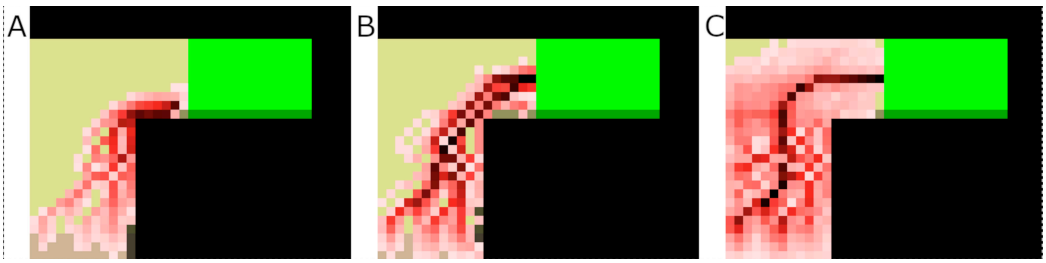

Figure A3. Aggregated probability of cell selection to the described paths for the corner tests, as based on the different values of the factors weights in Equation (A2) shown in Appendix C: (**A**) $\beta = 1$; (**B**) $\beta = 0.90$, $\delta = 0.10$; (**C**) $\alpha = 0.15$, $\beta = 0.70$, and $\delta = 0.15$. The green areas are the evacuation target in the access streets of the open space. The highest probability corresponds to the dark cells, while the lowest probability corresponds to the white cells.

References

1. Vecco, M. A Definition of Cultural Heritage: From the Tangible to the Intangible. *J. Cult. Herit.* **2010**, *11*, 321–324. [CrossRef]
2. UNESCO. *Recommendation on the Historic Urban Landscape*; UNESCO: Paris, France, 2021.
3. Cherfaoui, D.; Djelal, N. Change in Use and Development of Public Squares Considering Daily Temporalities. *Artic. Rev. Sci. Hum.* **2018**, *7*, 33–46. [CrossRef]

4. Stanley, B.W.; Stark, B.L.; Johnston, K.L.; Smith, M.E. Urban Open Spaces in Historical Perspective: A Transdisciplinary Typology and Analysis. *Urban Geogr.* **2012**, *33*, 1089–1117. [CrossRef]
5. Zakariya, K.; Harun, N.Z.; Mansor, M. Spatial Characteristics of Urban Square and Sociability: A Review of the City Square, Melbourne. *Procedia Soc. Behav. Sci.* **2014**, *153*, 678–688. [CrossRef]
6. Woo, G. Understanding the Principles of Terrorism Risk Modeling from Charlie Hebdo Attack in Paris. *Def. Terror. Rev.* **2015**, *7*, 33–46.
7. Cantatore, E.; Quagliarini, E.; Fatiguso, F. European Cities Prone to Terrorist Threats: Phenomenological Analysis of Historical Events towards Risk Matrices and an Early Parameterization of Urban Built Environment Outdoor Areas. *Sustainability* **2022**, *14*, 12301. [CrossRef]
8. Yang, Y.; Yu, J.; Wang, C.; Wen, J. Risk Assessment of Crowd-Gathering in Urban Open Public Spaces Supported by Spatio-Temporal Big Data. *Sustainability* **2022**, *14*, 6175. [CrossRef]
9. Quagliarini, E.; Bernardini, G.; Romano, G.; D'Orazio, M. Users' Vulnerability and Exposure in Public Open Spaces (Squares): A Novel Way for Accounting Them in Multi-Risk Scenarios. *Cities* **2023**, *133*, 104160. [CrossRef]
10. Julià, P.B.; Ferreira, T.M. From Single- to Multi-Hazard Vulnerability and Risk in Historic Urban Areas: A Literature Review. *Nat. Hazards* **2021**, *108*, 93–128. [CrossRef]
11. Villagràn De León, J.C. Vulnerability: A Conceptual and Methodological Review. *Res. Couns. Educ. Publ. Ser. UNU-EHS* **2006**, *64*, 540.
12. Paukaeva, A.A.; Setoguchi, T.; Luchkova, V.I.; Watanabe, N.; Sato, H. Impacts of the Temporary Urban Design on the People's Behavior—The Case Study on the Winter City Khabarovsk, Russia. *Cities* **2021**, *117*, 103303. [CrossRef]
13. Zomer, L.-B.; Schneider, F.; Ton, D.; Hoogendoorn-Lanser, S.; Duives, D.; Cats, O.; Hoogendoorn, S. Determinants of Urban Wayfinding Styles. *Travel Behav. Soc.* **2019**, *17*, 72–85. [CrossRef]
14. Han, S.; Song, D.; Xu, L.; Ye, Y.; Yan, S.; Shi, F.; Zhang, Y.; Liu, X.; Du, H. Behaviour in Public Open Spaces: A Systematic Review of Studies with Quantitative Research Methods. *Build. Environ.* **2022**, *223*, 109444. [CrossRef]
15. Gherri, B.; Maiullari, D.; Finizza, C.; Maretto, M.; Naboni, E. On the Thermal Resilience of Venetian Open Spaces. *Heritage* **2021**, *4*, 4286–4303. [CrossRef]
16. Lapkova, D.; Kotek, L.; Kralik, L. Soft Targets—Possibilities of Their Identification. In Proceedings of the 29th DAAAM International Symposium; Katalinic, B., Ed.; DAAAM International: Vienna, Austria, 2018; pp. 369–377.
17. *The European Commission Security by Design: Protection of Public Spaces from Terrorist Attacks*; Publications Office of the European Union: Luxembourg, 2022; ISBN 9789276419563. Available online: https://home-affairs.ec.europa.eu/news/security-design-protection-public-spaces-terrorist-attacks-2022-12-14_en (accessed on 25 June 2023).
18. Kalvach, Z. *Basics of Soft Targets Protection—Guidelines*, 2nd ed.; Soft Targets Protection Institute: Prague, Czech Republic, 2016.
19. Federal Emergency Management Agency. *FEMA 430: Site and Urban Design for Security: Guidance Against Potential Terrorist Attacks*; Federal Emergency Management Agency: Washington, DC, USA, 2007.
20. Karlos, V.; Larcher, M.; Solomos, G. *Review on Soft Target/Public Space Protection Guidance*; Publications Office of the European Union: Luxemburg, 2018; ISBN 978-92-79-79907-5.
21. Quagliarini, E.; Fatiguso, F.; Lucesoli, M.; Bernardini, G.; Cantatore, E. Risk Reduction Strategies against Terrorist Acts in Urban Built Environments: Towards Sustainable and Human-Centred Challenges. *Sustainability* **2021**, *13*, 901. [CrossRef]
22. FEMA. *Reference Manual to Mitigate Potential Terrorist Attacks Against Buildings*; FEMA: Washington, DC, USA, 2011; 510p.
23. Fischer, K.; Hiermaier, S.; Riedel, W.; Häring, I. Morphology Dependent Assessment of Resilience for Urban Areas. *Sustainability* **2018**, *10*, 1800. [CrossRef]
24. Bernardini, G.; Quagliarini, E. Terrorist Acts and Pedestrians' Behaviours: First Insights on European Contexts for Evacuation Modelling. *Saf. Sci.* **2021**, *143*, 105405. [CrossRef]
25. Booth, A.; Chmutina, K.; Bosher, L. Protecting Crowded Places: Challenges and Drivers to Implementing Protective Security Measures in the Built Environment. *Cities* **2020**, *107*, 102891. [CrossRef]
26. Pacheco Barzallo, A.; Fariña, J.; Álvarez de Andrés, E. Public Open Spaces: Enabling or Impeding Inclusive Evacuation during Disasters. *J. Public Space* **2022**, *7*, 79–92. [CrossRef]
27. Lin, J.; Zhu, R.; Li, N.; Becerik-Gerber, B. How Occupants Respond to Building Emergencies: A Systematic Review of Behavioral Characteristics and Behavioral Theories. *Saf. Sci.* **2020**, *122*, 104540. [CrossRef]
28. Zhu, R.; Lin, J.; Becerik-Gerber, B.; Li, N. Human-Building-Emergency Interactions and Their Impact on Emergency Response Performance: A Review of the State of the Art. *Saf. Sci.* **2020**, *127*, 104691. [CrossRef]
29. Pluchino, S.; Tribulato, C.M.G.; Caverzan, A.; Quillan, M.; Cimellaro, G.P.; Asce, M.; Mahin, S.; Asce, M. Agent-Based Model for Pedestrians ' Evacuation after a Blast Integrated with a Human Behavior Model. In Proceedings of the Structures Congress 2015, Reston, VA, USA, 23–25 April 2015; pp. 1506–1517.
30. Cheung, P.K.; Jim, C.Y. Improved Assessment of Outdoor Thermal Comfort: 1-Hour Acceptable Temperature Range. *Build. Environ.* **2019**, *151*, 303–317. [CrossRef]
31. Cadena, J.D.B.; Salvalai, G.; Bernardini, G.; Quagliarini, E. Determining Behavioural-Based Risk to SLODs of Urban Public Open Spaces: Key Performance Indicators Definition and Application on Established Built Environment Typological Scenarios. *Sustain. Cities Soc.* **2023**, *95*, 104580. [CrossRef]

32. Paolini, R.; Mainini, A.G.; Poli, T.; Vercesi, L. Assessment of Thermal Stress in a Street Canyon in Pedestrian Area with or without Canopy Shading. *Energy Procedia* **2014**, *48*, 1570–1575. [CrossRef]
33. Rosso, F.; Golasi, I.; Castaldo, V.L.; Piselli, C.; Pisello, A.L.; Salata, F.; Ferrero, M.; Cotana, F.; de Lieto Vollaro, A. On the Impact of Innovative Materials on Outdoor Thermal Comfort of Pedestrians in Historical Urban Canyons. *Renew. Energy* **2018**, *118*, 825–839. [CrossRef]
34. Haghani, M.; Kuligowski, E.; Rajabifard, A.; Lentini, P. Fifty Years of Scholarly Research on Terrorism: Intellectual Progression, Structural Composition, Trends and Knowledge Gaps of the Field. *Int. J. Disaster Risk Reduct.* **2022**, *68*, 102714. [CrossRef]
35. Liu, H.; Chen, H.; Hong, R.; Liu, H.; You, W. Mapping Knowledge Structure and Research Trends of Emergency Evacuation Studies. *Saf. Sci.* **2020**, *121*, 348–361. [CrossRef]
36. Wang, J.; Ni, S.; Shen, S.; Li, S. Empirical Study of Crowd Dynamic in Public Gathering Places during a Terrorist Attack Event. *Phys. Stat. Mech. Appl.* **2019**, *523*, 1–9. [CrossRef]
37. Arteaga, C.; Park, J.; Morris, B.T.; Sharma, S. Effect of Trained Evacuation Leaders on Victims' Safety during an Active Shooter Incident. *Saf. Sci.* **2023**, *158*, 105967. [CrossRef]
38. Zhang, F.; Wu, S.; Song, Z. Crowd Evacuation during Slashing Terrorist Attack: A Multi-Agent Simulation Approach. In Proceedings of the 2020 Winter Simulation Conference; Bae, K.-H., Feng, B., Kim, S., Lazarova-Molnar, S., Zheng, Z., Roeder, T., Thiesing, R., Eds.; Springer: Berlin/Heidelberg, Germany, 2020; pp. 206–217.
39. Chen, C.; Tong, Y.; Shi, C.; Qin, W. An Extended Model for Describing Pedestrian Evacuation under the Threat of Artificial Attack. *Phys. Lett. A* **2018**, *382*, 2445–2454. [CrossRef]
40. Liang, B.; van der Wal, C.N.; Xie, K.; Chen, Y.; Brazier, F.M.T.; Dulebenets, M.A.; Liu, Z. Mapping the Knowledge Domain of Soft Computing Applications for Emergency Evacuation Studies: A Scientometric Analysis and Critical Review. *Saf. Sci.* **2023**, *158*, 105955. [CrossRef]
41. Lu, P.; Zhang, Z.; Li, M.; Chen, D.; Yang, H. Agent-Based Modeling and Simulations of Terrorist Attacks Combined with Stampedes. *Knowl. Based Syst.* **2020**, *205*, 106291. [CrossRef]
42. Bernardini, G.; D'Orazio, M.; Quagliarini, E. Towards a "Behavioural Design" Approach for Seismic Risk Reduction Strategies of Buildings and Their Environment. *Saf. Sci.* **2016**, *86*, 273–294. [CrossRef]
43. Ronchi, E. Developing and Validating Evacuation Models for Fire Safety Engineering. *Fire Saf. J.* **2021**, *120*, 103020. [CrossRef]
44. Liu, R.; Jiang, D.; Shi, L. Agent-Based Simulation of Alternative Classroom Evacuation Scenarios. *Front. Archit. Res.* **2016**, *5*, 111–125. [CrossRef]
45. Song, Y.; Liu, B.; Li, L.; Liu, J. Modelling and Simulation of Crowd Evacuation in Terrorist Attacks. *Kybernetes* **2022**. *ahead-of-print*. [CrossRef]
46. Liu, Q. A Social Force Model for the Crowd Evacuation in a Terrorist Attack. *Phys. A Stat. Mech. Appl.* **2018**, *502*, 315–330. [CrossRef]
47. Li, S.; Zhuang, J.; Shen, S. A Three-Stage Evacuation Decision-Making and Behavior Model for the Onset of an Attack. *Transp. Res. Part C Emerg. Technol.* **2017**, *79*, 119–135. [CrossRef]
48. Yu, H.; Li, X.; Song, W.; Zhang, J.; Li, X.; Xu, H.; Jiang, K. Pedestrian Emergency Evacuation Model Based on Risk Field under Attack Event. *Phys. A Stat. Mech. Appl.* **2022**, *606*, 128111. [CrossRef]
49. D'Amico, A.; Russo, M.; Angelosanti, M.; Bernardini, G.; Vicari, D.; Quagliarini, E.; Currà, E. Built Environment Typologies Prone to Risk: A Cluster Analysis of Open Spaces in Italian Cities. *Sustainability* **2021**, *13*, 9457. [CrossRef]
50. Kurdi, H.A.; Al-Megren, S.; Althunyan, R.; Almulifi, A. Effect of Exit Placement on Evacuation Plans. *Eur. J. Oper. Res.* **2018**, *269*, 749–759. [CrossRef]
51. Santos, C.; Ferreira, T.M.; Vicente, R.; da Silva, J.R.M. Building Typologies Identification to Support Risk Mitigation at the Urban Scale—Case Study of the Old City Centre of Seixal, Portugal. *J. Cult. Herit.* **2013**, *14*, 449–463. [CrossRef]
52. Li, X.; Erpicum, S.; Mignot, E.; Archambeau, P.; Pirotton, M.; Dewals, B. Influence of Urban Forms on Long-Duration Urban Flooding: Laboratory Experiments and Computational Analysis. *J. Hydrol.* **2021**, *603*, 127034. [CrossRef]
53. Bernardini, G.; Romano, G.; Soldini, L.; Quagliarini, E. How Urban Layout and Pedestrian Evacuation Behaviours Can Influence Flood Risk Assessment in Riverine Historic Built Environments. *Sustain. Cities Soc.* **2021**, *70*, 102876. [CrossRef]
54. Mignot, E.; Li, X.; Dewals, B. Experimental Modelling of Urban Flooding: A Review. *J. Hydrol.* **2019**, *568*, 334–342. [CrossRef]
55. Zhu, Z.; Gou, L.; Liu, S.; Peng, D. Effect of Urban Neighbourhood Layout on the Flood Intrusion Rate of Residential Buildings and Associated Risk for Pedestrians. *Sustain. Cities Soc.* **2023**, *92*, 104485. [CrossRef]
56. Rozenfeld, M.; Givon, A.; Rivkind, A.; Bala, M.; Peleg, K.; Alfici, R.; Bahouth, H.; Becker, A.; Jeroukhimov, I.; Karawani, M.; et al. New Trends in Terrorism-Related Injury Mechanisms: Is There a Difference in Injury Severity? *Ann. Emerg. Med.* **2019**, *74*, 697–705. [CrossRef]
57. Banos, A.; Lang, C.; Marilleau, N. *Agent-Based Spatial Simulation with NetLogo*; Elsevier: Amsterdam, The Netherlands, 2015; 268p, ISBN 9780081007235.
58. Lu, P.; Li, M.; Zhang, Z. The Crowd Dynamics under Terrorist Attacks Revealed by Simulations of Three-Dimensional Agents. *Artif. Intell. Rev.* **2023**. [CrossRef]
59. van der Wal, C.N.; Formolo, D.; Robinson, M.A.; Minkov, M.; Bosse, T. Simulating Crowd Evacuation with Socio-Cultural, Cognitive, and Emotional Elements. *Lect. Notes Comput. Sci.* **2017**, *10*, 139–177. [CrossRef]

60. Blanco Cadena, J.D.; Caramia, M.; Salvalai, G.; Quagliarini, E. Using Digital Models of Built Environment Archetypes to Analyze and Communicate Climate Related Risk Outdoors. In *Rehabend 2022—9th Euro-American Congress on Construction Pathology, Rehabilitation Technology and Heritage Management*; Blanco, H., Bloffill, Y., Lombillo, I., Saez, M.P., Eds.; University of Cantabria—Circulo Rojo: Granada, Spain, 2022; pp. 1793–1802. ISBN 978-84-09-42253-1.
61. Wagner, N.; Agrawal, V. An Agent-Based Simulation System for Concert Venue Crowd Evacuation Modeling in the Presence of a Fire Disaster. *Expert Syst. Appl.* **2014**, *41*, 2807–2815. [CrossRef]
62. Yıldız, B.; Çağdaş, G. Fuzzy Logic in Agent-Based Modeling of User Movement in Urban Space: Definition and Application to a Case Study of a Square. *Build. Environ.* **2020**, *169*, 106597. [CrossRef]
63. Bernardini, G.; Ferreira, T.M. Emergency and Evacuation Management Strategies in Earthquakes: Towards Holistic and User-Centered Methodologies for Their Design and Evaluation. In *Seismic Vulnerability Assessment of Civil Engineering Structures at Multiple Scales*; Ferreira, T.M., Rodrigues, H., Eds.; Elsevier: Amsterdam, The Netherlands, 2022; pp. 275–321. ISBN 978-0-12-824071-7.
64. Montalbán Pozas, B.; Neila González, F.J. Housing Building Typology Definition in a Historical Area Based on a Case Study: The Valley, Spain. *Cities* **2018**, *72*, 1–7. [CrossRef]
65. Belpoliti, V.; Bizzarri, G.; Boarin, P.; Calzolari, M.; Davoli, P. A Parametric Method to Assess the Energy Performance of Historical Urban Settlements. Evaluation of the Current Energy Performance and Simulation of Retrofit Strategies for an Italian Case Study. *J. Cult. Herit.* **2018**, *30*, 155–167. [CrossRef]
66. Li, N.; Zhang, F.; Geng, W.; Li, Z. Research on Performance Improvement Design Strategies for Urban Historic Districts and Suburban Traditional Villages in Multiple Scopes. *J. Build. Eng.* **2023**, *72*, 106342. [CrossRef]
67. da Silva, F.T.; Reis, N.C.; Santos, J.M.; Goulart, E.V.; de Alvarez, C.E. Influence of Urban Form on Air Quality: The Combined Effect of Block Typology and Urban Planning Indices on City Breathability. *Sci. Total Environ.* **2022**, *814*, 152670. [CrossRef]
68. Dibble, J.; Prelorendjos, A.; Romice, O.; Zanella, M.; Strano, E.; Pagel, M.; Porta, S. On the Origin of Spaces: Morphometric Foundations of Urban Form Evolution. *Environ. Plan. B Urban Anal. City Sci.* **2019**, *46*, 707–730. [CrossRef]
69. Rashid, M. *The Geometry of Urban Layouts*; Springer: Cham, Switzerland, 2017; ISBN 978-3-319-30748-0.
70. Talen, E. In Support of the Unambiguous Neighborhood: A Proposed Size Typology. *J. Urban. Int. Res. Placemaking Urban Sustain.* **2018**, *11*, 480–502. [CrossRef]
71. Bassolino, E.; D'Ambrosio, V.; Sgobbo, A. Data Exchange Processes for the Definition of Climate-Proof Design Strategies for the Adaptation to Heatwaves in the Urban Open Spaces of Dense Italian Cities. *Sustainability* **2021**, *13*, 5694. [CrossRef]
72. Sharifi, E.; Lehmann, S. Correlation Analysis of Surface Temperature of Rooftops, Streetscapes and Urban Heat Island Effect: Case Study of Central Sydney. *J. Urban Environ. Eng.* **2015**, *9*, 3–11. [CrossRef]
73. Sharifi, A. Resilient Urban Forms: A Review of Literature on Streets and Street Networks. *Build. Environ.* **2019**, *147*, 171–187. [CrossRef]
74. Choi, Y.; Yoon, H.; Kim, D. Where Do People Spend Their Leisure Time on Dusty Days? Application of Spatiotemporal Behavioral Responses to Particulate Matter Pollution. *Ann. Reg. Sci.* **2019**, *63*, 317–339. [CrossRef]
75. Liu, P. The Effect of Temperature on Outdoor Recreation Activities: Evidence from Visits to Federal Recreation Sites. *Environ. Res. Lett.* **2022**, *17*, 044037. [CrossRef]
76. Diffey, B.L. An Overview Analysis of the Time People Spend Outdoors. *Br. J. Dermatol.* **2011**, *164*, 848–854. [CrossRef] [PubMed]
77. Speak, A.F.; Salbitano, F. Summer Thermal Comfort of Pedestrians in Diverse Urban Settings: A Mobile Study. *Build. Environ.* **2022**, *208*, 108600. [CrossRef]
78. Ludvigsen, J.A.L.; Millward, P. A Security Theater of Dreams: Supporters' Responses to "Safety" and "Security" Following the Old Trafford "Fake Bomb" Evacuation. *J. Sport Soc. Issues* **2020**, *44*, 3–21. [CrossRef]
79. Bruyelle, J.-L.; O'Neill, C.; El-Koursi, E.-M.; Hamelin, F.; Sartori, N.; Khoudour, L. Improving the Resilience of Metro Vehicle and Passengers for an Effective Emergency Response to Terrorist Attacks. *Saf. Sci.* **2014**, *62*, 37–45. [CrossRef]
80. Lovreglio, R.; Ngassa, D.-C.; Rahouti, A.; Paes, D.; Feng, Z.; Shipman, A. Prototyping and Testing a Virtual Reality Counterterrorism Serious Game for Active Shooting. *SSRN Electron. J.* **2021**, *82*, 103283. [CrossRef]
81. Liu, Q. A Social Force Approach for the Defensive Strategy of Security Guards in a Terrorist Attack. *Int. J. Disaster Risk Reduct.* **2020**, *46*, 101605. [CrossRef]
82. Lu, P.; Li, Y.; Wen, F.; Chen, D. Agent-Based Modeling of Mass Shooting Case with the Counterforce of Policemen. *Complex Intell. Syst.* **2023**. [CrossRef]
83. Lu, P.; Wen, F.; Li, Y.; Chen, D. Multi-Agent Modeling of Crowd Dynamics under Mass Shooting Cases. *Chaos Solitons Fractals* **2021**, *153*, 111513. [CrossRef]
84. Lu, P.; Zhang, Z.; Li, M. Individual Heights and Phase Transition under Crowd Emergencies: Agent-Based Modeling from 2 to 3D. *Artif. Intell. Rev.* **2023**. [CrossRef]
85. Kebir, O.; Nouaouri, I.; Rejab, L.; Ben Said, L. Simulating Actors' Behaviors within Terrorist Attacks Scenarios Based on a Multi-Agent System. In Proceedings of the 12th International Defense and Homeland Security Simulation Workshop, Rome, Italy, 19–21 September 2022.
86. Ronchi, E.; Kuligowski, E.D.; Reneke, P.A.; Peacock, R.D.; Nilsson, D. *The Process of Verification and Validation of Building Fire Evacuation Models*; National Institute of Standards and Technology: Gaithersburg, MD, USA, 2013; Volume 1822.
87. Li, Y.; Chen, M.; Dou, Z.; Zheng, X.; Cheng, Y.; Mebarki, A. A Review of Cellular Automata Models for Crowd Evacuation. *Phys. A Stat. Mech. Appl.* **2019**, *526*, 120752. [CrossRef]

88. Bosina, E.; Weidmann, U. Estimating Pedestrian Speed Using Aggregated Literature Data. *Phys. A Stat. Mech. Appl.* **2017**, *468*, 1–29. [CrossRef]
89. EM-DAT EM-DAT Database. Available online: https://www.emdat.be/database (accessed on 1 December 2022).
90. Wilensky, U.; Rand, W. *An Introduction to Agent-Based Modeling. Modeling Natural, Social, and Engineered Complex Systems with NetLogo*; MIT Press: Cambridge, MA, USA, 2015; ISBN 978-0-262-73189-8.
91. Banerjee, A.; Maurya, A.K.; Lämmel, G. Pedestrian Flow Characteristics and Level of Service on Dissimilar Facilities: A Critical Review. *Collect. Dyn.* **2018**, *3*, A17. [CrossRef]
92. Gravetter, F.J.; Wallnan, L.B. *Statistics for the Behavioural Sciences*, 9th ed.; Cengage Learning: Wadsworth, OH, USA, 2013; ISBN 9781111830991.
93. Hassanpour, S.; Rassafi, A.A. Agent-Based Simulation for Pedestrian Evacuation Behaviour Using the Affordance Concept. *KSCE J. Civ. Eng.* **2021**, *25*, 1433–1445. [CrossRef]
94. Roan, T.-R.; Haklay, M.; Ellul, C. Modified Navigation Algorithms in Agent-Based Modelling for Fire Evacuation Simulation. In Proceedings of the 11th International Conference GeoComputation, London, UK, 20–22 July 2011; pp. 43–49.
95. Kang, P.; Lv, Y.; Deng, Q.; Liu, Y.; Zhang, Y.; Liu, X.; Zhang, L. Investigating Lushan Earthquake Victims' Individual Behavior Response and Rescue Organization. *Int. J. Environ. Res. Public Health* **2017**, *14*, 1556. [CrossRef] [PubMed]
96. Lakoba, T.I.; Kaup, D.J.; Finkelstein, N.M. Modifications of the Helbing-Molnár-Farkas-Vicsek Social Force Model for Pedestrian Evolution. *Simulation* **2005**, *81*, 339–352. [CrossRef]
97. Xiao, Q.; Li, J. Evacuation Model of Emotional Contagion Crowd Based on Cellular Automata. *Discret. Dyn. Nat. Soc.* **2021**, *2021*, 1–18. [CrossRef]
98. Li, X.; Guo, F.; Kuang, H.; Geng, Z.; Fan, Y. An Extended Cost Potential Field Cellular Automaton Model for Pedestrian Evacuation Considering the Restriction of Visual Field. *Phys. A Stat. Mech. Appl.* **2019**, *515*, 47–56. [CrossRef]